Cell Reports
Medicine

Article

Caspase-8 inhibition improves the outcome of bacterial infections in mice by promoting neutrophil activation

Graphical abstract

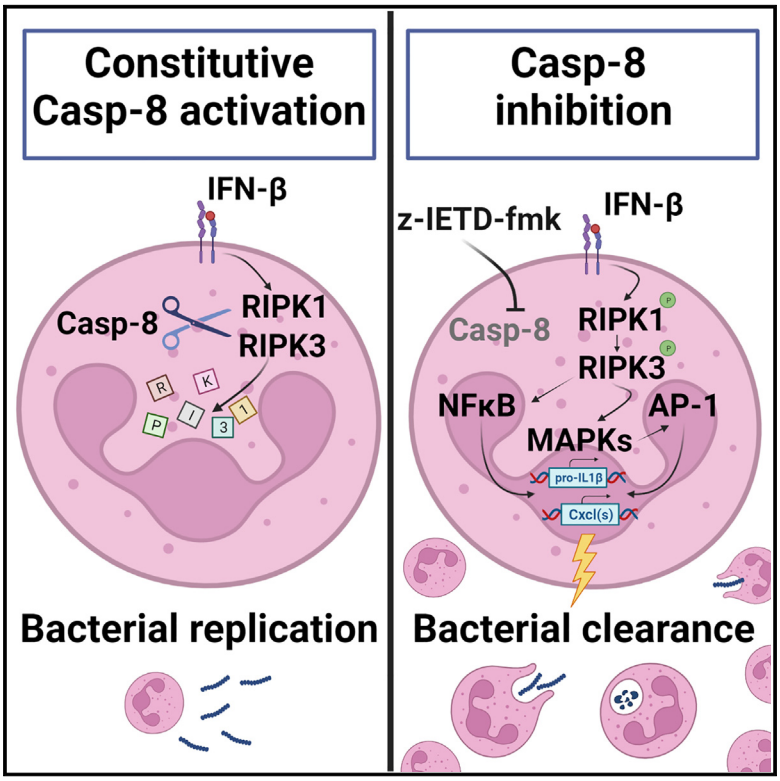

Authors

Germana Lentini, Agata Famà, Giuseppe Valerio De Gaetano, ..., Terje Espevik, Concetta Beninati, Giuseppe Teti

Correspondence

gioteti@mac.com

In brief

Caspase-8 prevents inflammation during homeostasis, but the underlying mechanisms are unclear. Lentini et al. show that caspase-8 negatively regulates—in neutrophils—a spontaneous pro-inflammatory pathway driven by the RIPK3 kinase and sustained by interferon-β. By unleashing this pathway, pharmacological caspase-8 inhibition induces neutrophil mobilization and can effectively treat bacterial infections.

Highlights

- Caspase-8 controls a constitutively activated inflammatory pathway in neutrophils
- This pathway is dependent on tonic IFN-β production and RIPK3 but not MLKL
- Caspase-8 inhibition induces chemokine production and neutrophil recruitment
- Caspase-8 inhibition has therapeutic effects against lethal bacterial infection

Lentini et al., 2023, Cell Reports Medicine *4*, 101098
July 18, 2023
https://doi.org/10.1016/j.xcrm.2023.101098

CellPress

Cell Reports Medicine

CellPress
OPEN ACCESS

Article

Caspase-8 inhibition improves the outcome of bacterial infections in mice by promoting neutrophil activation

Germana Lentini,[1,7] Agata Famà,[1,7] Giuseppe Valerio De Gaetano,[1,2] Francesco Coppolino,[3] Ahlem Khachroub Mahjoub,[1] Liv Ryan,[4] Egil Lien,[4,5] Terje Espevik,[4] Concetta Beninati,[1,2,6] and Giuseppe Teti[2,6,8,*]

[1]Department of Human Pathology, University of Messina, Messina, Italy
[2]Scylla Biotech Srl, Messina, Italy
[3]Department of Chemical, Biological and Pharmaceutical Sciences, University of Messina, Messina, Italy
[4]Centre of Molecular Inflammation Research, Department of Cancer Research and Molecular Medicine, Norwegian University of Science and Technology, Trondheim, Norway
[5]Division of Infectious Diseases and Immunology, Program in Innate Immunity, Department of Medicine, University of Massachusetts Chan Medical School, Worcester, MA, USA
[6]Senior author
[7]These authors contributed equally
[8]Lead contact
*Correspondence: gioteti@mac.com
https://doi.org/10.1016/j.xcrm.2023.101098

SUMMARY

During differentiation, neutrophils undergo a spontaneous pro-inflammatory program that is hypothesized here to be under caspase-8 control. In mice, intraperitoneal administration of the caspase-8 inhibitor z-IETD-fmk is sufficient to unleash the production of pro-inflammatory cytokines and neutrophil influx in the absence of cell death. These effects are due to selective inhibition of caspase-8 and require tonic interferon-β (IFN-β) production and RIPK3 but not MLKL, the essential downstream executioner of necroptotic cell death. *In vitro*, stimulation with z-IETD-fmk is sufficient to induce significant cytokine production in murine neutrophils but not in macrophages. Therapeutic administration of z-IETD-fmk improves clinical outcome in models of lethal bacterial peritonitis and pneumonia by augmenting cytokine release, neutrophil influx, and bacterial clearance. Moreover, the inhibitor protects mice against high-dose endotoxin shock. Collectively, our data unveil a RIPK3- and IFN-β-dependent pathway that is constitutively activated in neutrophils and can be harnessed therapeutically using caspase-8 inhibition.

INTRODUCTION

Caspases constitute a group of conserved proteases that play fundamental roles in cell differentiation and homeostasis, including organismal development and host responses to tissue damage.[1] The substrate specificity of each caspase type is mostly determined by the amino acid sequence preceding the aspartate residue in the substrate cleavage site.[2] Caspase-8 is strategically located at the intersection of several pathways that are initiated by death receptors and other innate immune receptors, leading to inflammatory responses and/or to the execution of cell death programs, including apoptosis, pyroptosis, and necroptosis.[3,4] Caspase-8 activation has widely divergent effects depending on the cell type, activating stimulus, and modulation of its enzymatic activities by interaction with different molecular partners.[5] After signaling by death receptors, caspase-8 can become activated by homo-dimerization and auto-processing, leading to apoptosis, a predominantly non-inflammatory form of cell death. However, caspase-8 can also promote pyroptosis, an inflammatory form of cell death, either by activating inflammatory caspases, such as caspase 1, or by directly processing caspase-1 substrates such as gasdermin D, interleukin 1β (IL-1β), and IL-18.[6,7] Moreover, caspase-8 can prevent necroptosis, also an inflammatory form of cell death, by enzymatically inactivating crucial necroptosis mediators, such as RIPK1 and RIPK3.[8,9] Genetic defects of caspase-8 in humans are associated with increased susceptibility to bacterial respiratory and herpesvirus infections[10] as well as very early onset colitis.[11] Despite its ability to promote the expression of pro-inflammatory genes in macrophages in response to infectious agents,[12–18] caspase-8 appears to downregulate inflammation in the context of tissue homeostasis and development.[5] Indeed, localized deletion of caspase-8 or its expression in an enzymatically defective form results in marked inflammatory changes in various types of tissues.[19] The mechanisms regulating these effects are incompletely characterized but are often linked to the ability of caspase-8 to inhibit inflammatory cell death, including necroptosis.

Pathogen resistance to antimicrobial drugs, which have been a mainstay of modern medicine for the last eight decades, is a major public health threat. The persisting burden of community-acquired

and nosocomial infections causes our continuing dependence on antimicrobials, which maintain a strong selective pressure and lead to further increases in antimicrobial resistance.[20] To interrupt this vicious circle, it is essential to develop effective anti-infectious treatments, such as host-directed therapies, that do not impose a selective pressure on microorganisms. Neutrophils represent the first and most effective line of defense against bacterial and fungal infections deployed by the immune system.[21,22] In a highly ordered, sequential process of cell differentiation in the bone marrow, maturing neutrophils upregulate the expression of genes encoding for ligand-receptor pairs and signaling molecules involved in caspase-8 activation.[23] Intriguingly, upregulation of this pathway coincides in time with increased expression of interferon-dependent and pro-inflammatory genes, the latter including *Il1b*, *Ccl6*, and *Csf3R*.[23,24] Therefore, we hypothesized that during their differentiation into mature forms, neutrophils constitutively activate a pro-inflammatory program that is sustained by type I interferon (IFN) and regulated by caspase-8. We identify here a necroptosis-independent inflammatory pathway that is spontaneously activated in neutrophils, is held in check by caspase-8, and is dependent on RIPK1/3, caspase-1, and IFN-β. This pathway can be exploited therapeutically, as shown by the ability of pharmacological caspase-8 inhibition to promote chemokine production, neutrophil migration, bacterial clearance, and, at the same time, endotoxin resistance.

RESULTS

z-IETD-fmk promotes clearance of lethal bacterial infection

Because genetic inactivation of caspase-8 can produce inflammation in various types of tissues,[3] we asked whether pharmacological caspase-8 inhibition could augment neutrophil responses in the context of bacterial infection and promote pathogen clearance. To test this, mice were given the caspase-8 inhibitor z-IETD-fmk at a dose that was found in preliminary experiments to inhibit *in vivo* activation of caspase-8 but not caspase-1 (see STAR Methods). After 4 h, mice were challenged intraperitoneally (i.p.) with a highly lethal dose of group B streptococcus (GBS), an important agent of sepsis and meningitis that has been used over the years to model antibacterial innate immune responses.[25–28] In control animals, which consisted of mice treated with saline or with the DMSO vehicle, GBS rapidly grew during the first hour post-challenge and persisted at elevated numbers in the peritoneal cavity (Figure 1A). In contrast, bacterial numbers quickly declined in animals treated with z-IETD-fmk, reaching levels that were 4–5 orders of magnitude lower than those of control mice (Figures 1A and 1B). Inhibitor-treated animals completely cleared infection by 5 h post-challenge (Figure 1A) and remained in good health thereafter, while all control animals showed signs of irreversible disease and were humanely euthanized (Figures S1A–S1C). The protective effect of z-IETD-fmk was not due to direct antibacterial activity since this compound did not affect *in vitro* GBS growth at concentrations up to 2 mg/mL (Figure S1D). The early decline in bacterial numbers observed in IETD-treated mice was coincident in timing with the influx of neutrophils into the peritoneal cavity and the release of pro-inflammatory cytokines and chemokines (Figures 1C–1G) in the absence of increased cell death over that observed in control mice (Figures 1H and 1I).

Since IETD may cross-inhibit other caspases in addition to caspase-8,[29] we compared the z-IETD-fmk effects with those of other caspase inhibitors, such as the pan-caspase inhibitor z-VAD-fmk and the caspase-1 inhibitor z-YVAD-fmk. However, both z-VAD-fmk and YVAD-fmk were ineffective at reducing bacterial burden or at increasing neutrophil influx (Figures S1E–S1H). Collectively, these data indicate that treatment with the caspase-8 inhibitor z-IETD-fmk, but not with pan-caspase or caspase-1 inhibitors, potentiates the production of pro-inflammatory cytokines and chemokines in a cell death-independent manner, resulting in increased neutrophil recruitment and containment of lethal bacterial infection.

z-IETD-fmk administration is sufficient to induce inflammatory changes *in vivo*

We next investigated whether z-IETD-fmk could produce pro-inflammatory changes by itself, in the absence of infection or other external stimuli, by analyzing peritoneal lavage fluid (PLF) samples obtained at different times after i.p. inoculation with the compound. Significant cytokine/chemokine elevations were measured as early as 1 (Cxcl1 and 2), 2 (IL-1β and IL-18), and 3 h (IL-1α) after treatment, while their levels were low or undetectable in samples from vehicle-treated mice (Figures 2A–2E) or from mice treated with the pan-caspase inhibitor z-VAD-fmk (Figure S2A). Cytokine production occurred in the absence of detectable cell death since no significant decrease in peritoneal cell viability occurred over 5 h after administration of z-IETD-fmk (Figure S1I). Cytokine appearance was preceded by activation of selected cytokine genes (Figure S2B) and was concomitant in timing with neutrophil recruitment into the peritoneal cavity (Figure 2F). These effects were not due to endotoxin contamination since endotoxin levels in the z-IETD-fmk preparations employed were <0.01 EU/mL. Further analysis of PLF supernatants using a protein array revealed that z-IETD-fmk induced the release of a range of chemokines, cytokines, and growth factors, including CCL2, CCL12, Cxcl1/2/10/12/13, IL-16, IL-17, G-CSF, and M-CSF, as well as the complement component C5a and the metalloproteinase inhibitor TIMP-1 (Figure 2G; Table S1). These data indicate that z-IETD-fmk administration is, by itself, sufficient to induce transcriptionally regulated inflammatory changes *in vivo*, including the production of a distinctive pattern of pro-inflammatory cytokines and neutrophil-attracting chemokines, as well as neutrophil recruitment.

z-IETD-fmk induces pro-inflammatory cytokine production in neutrophils but not in macrophages

Next, it was of interest to assess whether z-IETD-fmk could induce cytokine production not only *in vivo* but also *in vitro*. Indeed, significant Cxcl1 and IL-1β elevations were detected in unseparated peritoneal cells cultured overnight in the presence of 50 μM z-IETD-fmk (Figure 3A) and in bone marrow cells, albeit at lower levels (Figure 3B). However, Cxcl1 or IL-1β production could not be induced by z-IETD-fmk treatment in cultures of mouse macrophages isolated from a variety of sources, in macrophage cell lines, or in mast cells (Figures S2C and S2D;

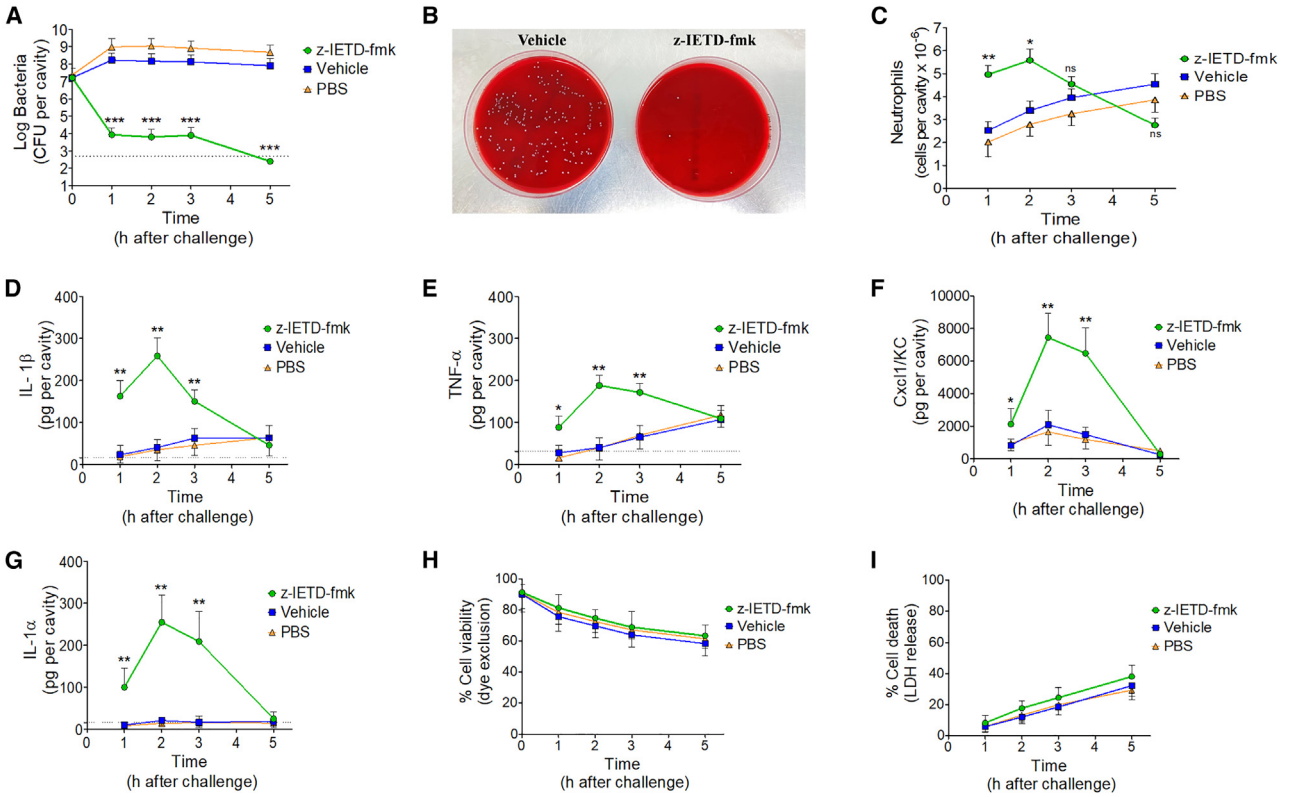

Figure 1. Caspase-8 inhibition promotes bacterial clearance

Mice were injected i.p. with 0.2 mL PBS, vehicle (7.5% dimethyl sulfoxide in PBS), or the caspase-8 inhibitor z-IETD-fmk (6 mg/kg) at 4 h before i.p. challenge with 4×10^7 CFU GBS per mouse. PLF samples were collected at the indicated times after bacterial challenge and analyzed.

(A) Bacterial numbers in PLF samples.

(B) Blood agar plates showing bacterial colonies after seeding PLF samples obtained at 2 h after challenge.

(C) Neutrophil counts.

(D–G) Cytokine concentrations.

(H) Cell viability.

(I) LDH release.

Shown are means + SD. The dashed lines indicate the limits of detection of the tests. Shown are cumulative data from two experiments, each involving 4 animals per group. *$p < 0.05$; **$p < 0.01$; ***$p < 0.001$ versus vehicle-treated mice, as determined by the Mann-Whitney U test; ns, not significant.

data not shown). Notably, increased transcription of IL-1β and tumor necrosis factor-α (TNF-α) genes (Figures S3A and S3B) and cytokine release (Figure 3C) was detected in murine bone marrow neutrophils, but not in macrophages, in the presence of z-IETD-fmk. Moreover, production of CXCL8 and MIP-1α was detected in human blood after the addition of z-IETD-fmk (Figure S3C).

Since neutrophils spontaneously undergo apoptosis during *in vitro* culture,[22] it was of interest to ascertain whether perturbed patterns of cell death might have contributed to the IETD effects. Culture for 24 h in the presence of z-IETD-fmk slightly increased spontaneous cell death in neutrophils (Figure S4A). This increase in cell death was not due to necroptosis since it was not prevented by the lack of the pseudokinase MLKL, the essential executioner of necroptosis (Figure S4A). Increased cell death was not responsible for IETD-induced cytokine release since the latter could be observed even at times (e.g., at 6–8 h after stimulation) at which cell viability was high and similar in z-IETD-fmk- and vehicle-treated neutrophils (Figure S4B).

In further experiments, we found that neutrophils were required for IETD-induced *in vivo* production of cytokines and chemokines since significant cytokine elevations could not be detected in mice depleted of neutrophils by anti-Ly6G antibody treatment prior to i.p. injection with z-IETD-fmk (Figure S4C). Moreover, cytokine elevations were not detected in peritoneal cells obtained from neutrophil-depleted mice after *in vitro* stimulation with IETD (Figure S4D). To gain further insights into the cell types and mechanisms involved in z-IETD-fmk-induced cytokine production, we stained peritoneal cells obtained at various times after i.p. administration of z-IETD-fmk for intracellular immunoreactive IL-1β, used as a marker for cytokine-producing cells. Immunoreactive IL-1β was detected in 1%–2% of peritoneal cells obtained from mice inoculated with vehicle (Figures 4A and S5A) or PBS or from untreated mice (data not shown). After z-IETD-fmk treatment, the number of IL-1β-producing cells increased concomitantly with neutrophil influx, and at 4 h, neutrophils and macrophages represented 60%–70% and 10%–20%, respectively, of the IL-1β-producing cells (Figure 4A).

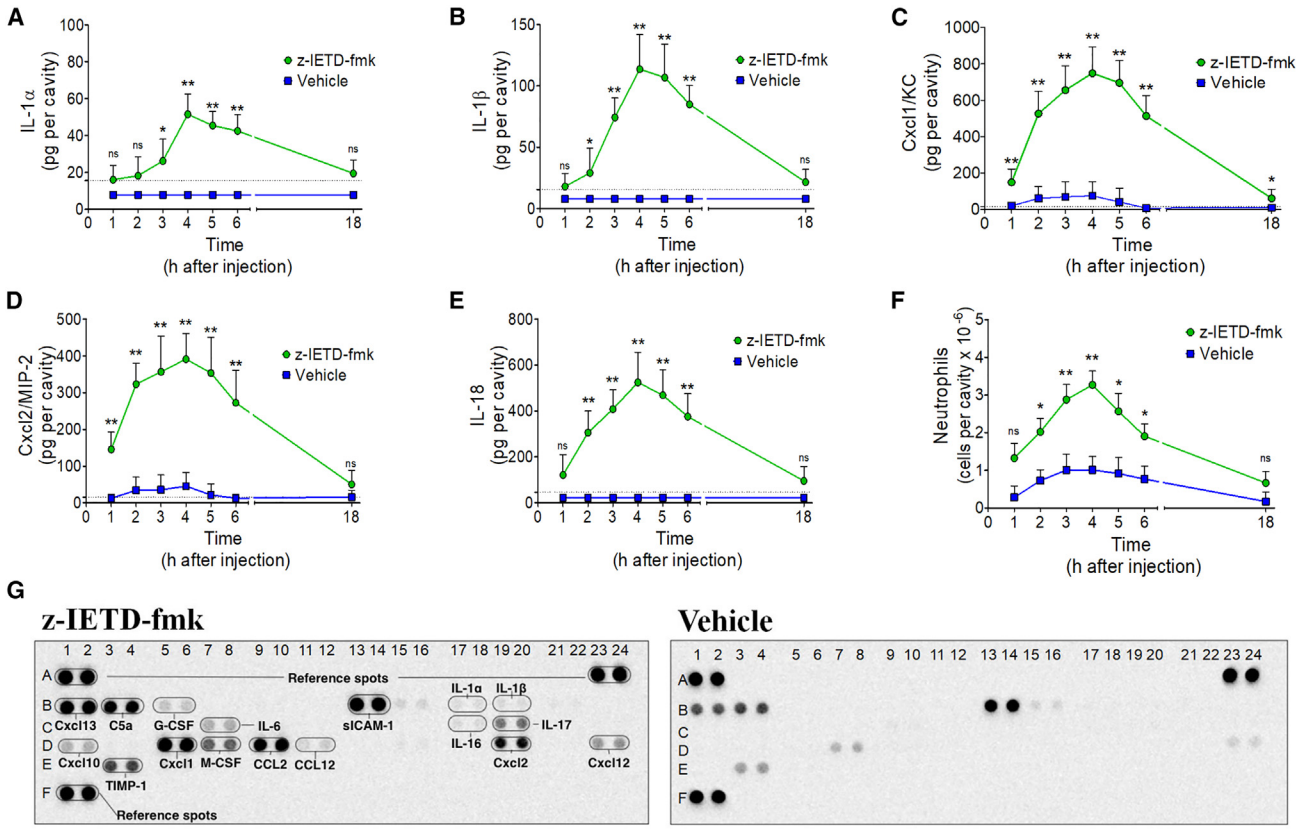

Figure 2. Treatment with z-IETD-fmk is sufficient to induce inflammation *in vivo*

(A–E) Cytokine concentrations in PLF samples obtained from mice treated with z-IETD-fmk (6 mg/kg, i.p.) or vehicle for the indicated times in the absence of other stimuli.

(F) Kinetics of neutrophil influx in the peritoneal cavity after treatment with z-IETD-fmk. Each determination was conducted on a different animal in the course of one experiment involving five animals per group. Shown in (A–F) are means + SD. The dashed lines indicate the limits of detection of the tests. *$p < 0.05$; **$p < 0.01$ versus vehicle-treated mice, as determined by the Mann-Whitney U test; ns, not significant.

(G) Mouse cytokine array analysis of PLF samples collected at 4 h after treatment with the caspase-8 inhibitor z-IETD-fmk (6 mg/kg i.p.; left) or vehicle (right) in the absence of other stimuli. Data are from one representative experiment of three showing similar results. A list of the cytokines and other mediators tested in (G) and their coordinates in the array is provided in Table S1.

Collectively these data indicate that neutrophils are activated both *in vitro* and *in vivo* by z-IETD-fmk and represent most of the cells producing IL-1β cells after i.p. treatment with the inhibitor.

Caspase-1/-11 are involved in z-IETD-induced IL-1β production

Next, we aimed at obtaining insights into the molecular mechanisms underlying z-IETD-fmk-induced inflammation using mice lacking key signaling proteins involved in cytokine responses and programmed cell death. First, we sought to formally confirm that IETD produces its effects by specifically acting on caspase-8. To this end, we used mice lacking both caspase-8 and MLKL, the essential executioner of necroptotic cell death, since the isolated absence of caspase 8 is embryonically lethal due to uncontrolled necroptosis.[3] Notably, IETD-induced neutrophil recruitment and IL-1β production were completely abrogated in mice lacking both caspase-8 and MLKL, but not in those lacking just MLKL, confirming that the IETD effects are specifically linked to inhibition of caspase-8 (Figure 4B). Next, we showed that Toll-like receptors (TLRs) and their agonists, which can potently induce pro-inflammatory changes, are not involved in the z-IETD-fmk effects, as evidenced by robust responses to the inhibitor in mice lacking the TLR adaptors Myd88 or TRIF (Figure S5B). Since expression of enzymatically inactive caspase-8 is sufficient to activate a caspase-1/-11-dependent inflammasome in the intestine,[19,30] we next investigated whether combined deletion of caspase-1 and caspase-11 would affect z-IETD-fmk-induced responses. The absence of caspase-1 and -11, but not NLRP3, led to significant reductions in IL-1β and IL-18 levels as well as in the numbers of neutrophils and IL-1β-producing cells after z-IETD-fmk treatment (Figures 5B–5E and S5). Moreover, transcription of pro-IL1-β mRNA was significantly decreased in peritoneal cells lacking caspase-1/-11 after z-IETD-fmk treatment (Figure S6A).

Partially processed IL-1β was detected in peritoneal cells from wild-type mice after i.p. administration of z-IETD-fmk, and such processing was reduced in caspase-1/-11 double-knockout

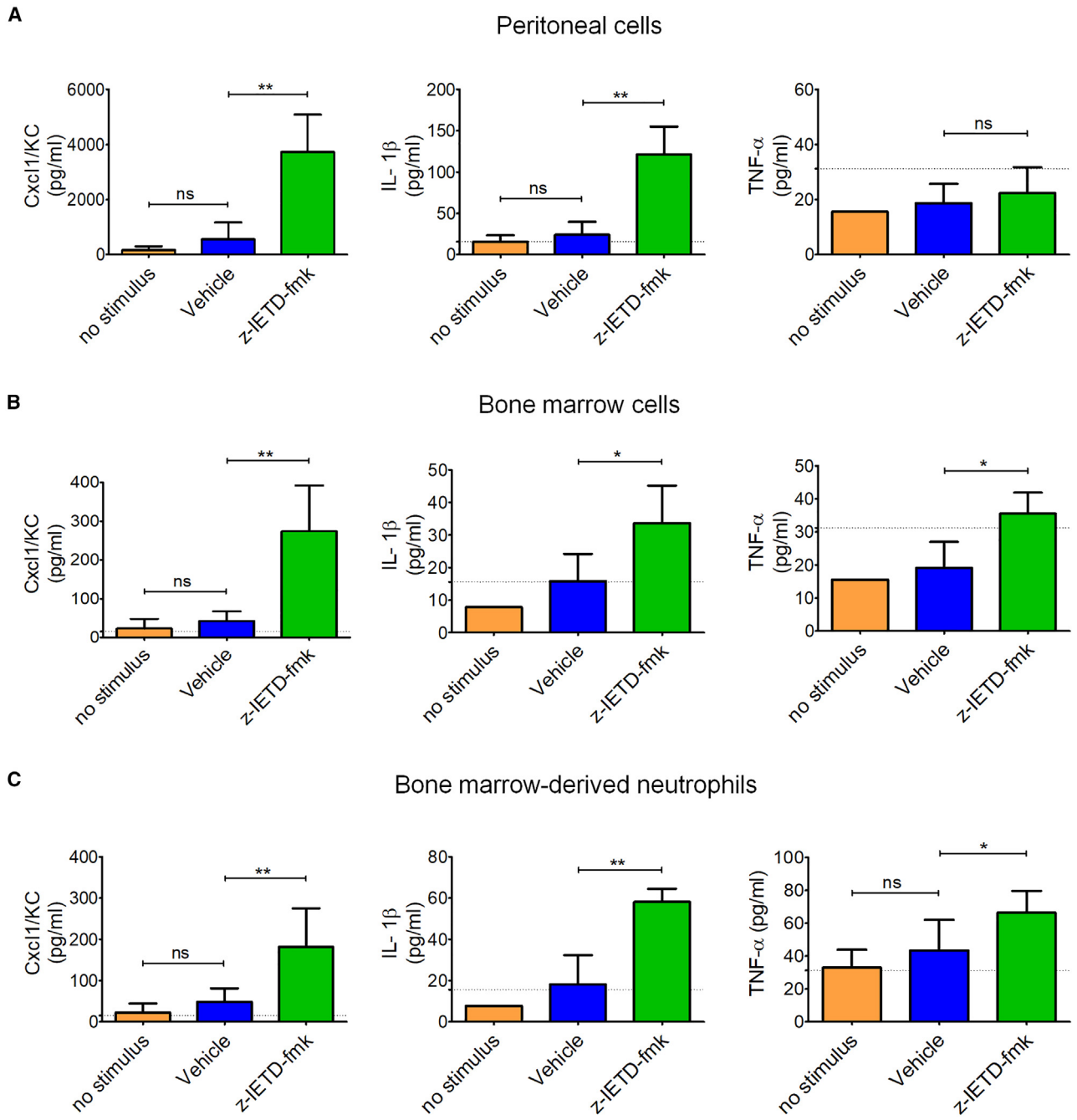

Figure 3. z-IETD-fmk stimulates inflammatory cytokine release in *in vitro* cultured neutrophils

Cytokine concentrations in supernatants from total peritoneal cells (A), total bone marrow cells (B), or neutrophils separated from bone marrow cells by density gradient centrifugation (C). All cells were cultured overnight in the presence of z-IETD-fmk (50 μM) or vehicle. Shown are means + SD from five independent experiments conducted in duplicate. *p < 0.05; **p < 0.01, as determined by the Mann-Whitney U test; ns, not significant.

(KO) animals (Figure 5A). Residual IL-1β processing in these animals after z-IETD-fmk treatment was possibly related to the activities of neutrophil serine proteases.[31] Notably, z-IETD administration was unable to reduce bacterial burden in GBS-challenged caspase-1/-11 double-KO mice (Figure S6B), and co-administration of the caspase 1/11 inhibitor z-YVAD-fmk in wild-type mice abrogated the beneficial effects on infection observed when z-IETD-fmk was given alone (Figure S6C). Collectively, these data indicate that caspase-1 or -11 or both, but not NLRP3, make a significant contribution to the inflammatory changes induced by z-IETD-fmk *in vivo*. Moreover, abrogation of the protective effects of z-IETD-fmk by caspase-1

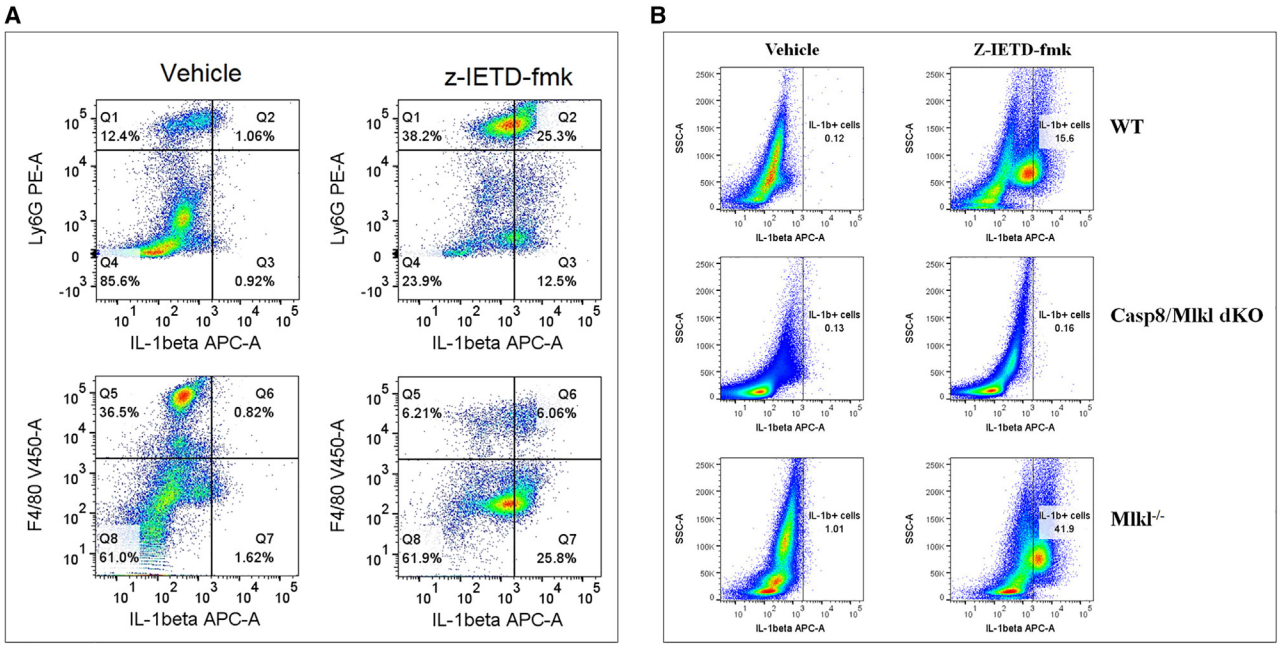

Figure 4. Neutrophils are a major source of IL-1β in response to z-IETD-fmk

Representative flow cytometry plots showing cells positive for intracellular IL-1β staining (APC+ cells) in PLF samples obtained from mice after treatment with z-IETD-fmk (6 mg/kg, i.p.) in the absence of other stimuli.

(A) Peritoneal cells were collected at 4 h after administration of vehicle or z-IETD-fmk. Neutrophils and macrophages were identified based on expression of Ly6G (PE+) and F4/80 (V450+), respectively. Data are from one representative experiment of three producing similar results.

(B) Peritoneal cells from mice lacking caspase-8 and MLKL (Casp8/Mlkl double KO) or mice lacking just MLKL (*Mlkl*$^{-/-}$) were collected at 3 h after administration of z-IETD-fmk or vehicle. Data are from one representative experiment of three producing similar results.

inhibition provided an explanation for the previously observed ineffectiveness of pan-caspase inhibition to promote bacterial clearance (Figure S1E).

z-IETD-induced inflammation requires IFN-β and RIPK3 but not MLKL

Next, we asked whether necroptosis, which requires RIPK1-dependent activation of RIPK3 and MLKL, was involved in the *in vivo* inflammatory response triggered by caspase-8 inhibition. Phosphorylation of RIPK1was detected by western blot in lysates of peritoneal cells obtained after i.p. administration of z-IETD-fmk (Figure 6A). Pretreatment with the RIPK1 kinase-inhibitor necrostatin-1 significantly attenuated IETD-induced pro-inflammatory changes (Figures 6B–6D), while these were completely abrogated by the absence of RIPK3 (Figure 6E). In contrast, the number of IL-1β+ cells (Figure 6E) and pro-IL-1β transcription (Figure S6D) were increased in necroptosis-deficient mice lacking MLKL. Because several type I IFN-dependent genes become activated synchronously with the IL-1β gene during neutrophil development,[24] we asked whether z-IETD-induced IL-1β transcription depended on type I IFN production. This seemed indeed to be the case since transcription of IL-1β, as well as Cxcl1, was totally abrogated in peritoneal cells obtained from *IFN-β*$^{-/-}$mice after i.p. treatment with z-IETD-fmk, and this effect was reversed by treatment with recombinant IFN-β (Figures S6E–S6H). Moreover, baseline levels of mRNA transcripts encoding for caspase-8 and -1 and RIPK1, but not RIPK3, were reduced in cells lacking IFN-β, and such levels were increased by IFN-β treatment (Figure S6I). Collectively these data indicate that the pro-inflammatory effects of z-IETD-fmk are driven by a RIPK3-dependent mechanism that is partially kept under control by MLKL. Moreover, responsiveness to z-IETD-fmk depends on tonic IFN-β production, which might be required for maintaining baseline levels of RIPK1 and caspase-8 and -1 expression.

Protective effects of caspase-8 inhibition in septic shock and bacterial infection models

Excessive pro-inflammatory cytokine production can have detrimental consequences for the outcome of infections, particularly in the context of sepsis.[27,32,33] Since z-IETD-fmk treatment induced here robust pro-inflammatory cytokine responses, we ascertained whether such treatment is detrimental in septic shock models. Lipopolysaccharide (LPS), or endotoxin, is a crucial contributor to septic shock caused by gram-negative bacteria in humans, and this shock form can be modeled in mice by high-dose LPS challenge. Strikingly, z-IETD-fmk treatment largely prevented hypothermia and death induced by high-dose endotoxin, despite producing moderate elevations in TNF-α and IL-β blood levels (Figure 7A). Similarly, z-IETD-fmk treatment significantly protected mice in a gram-positive shock model involving the i.v. administration of live GBS bacteria[34,35] by inducing moderate elevations in cytokine blood levels and reducing bacterial burden (Figures S7A, S7B, S7G, and

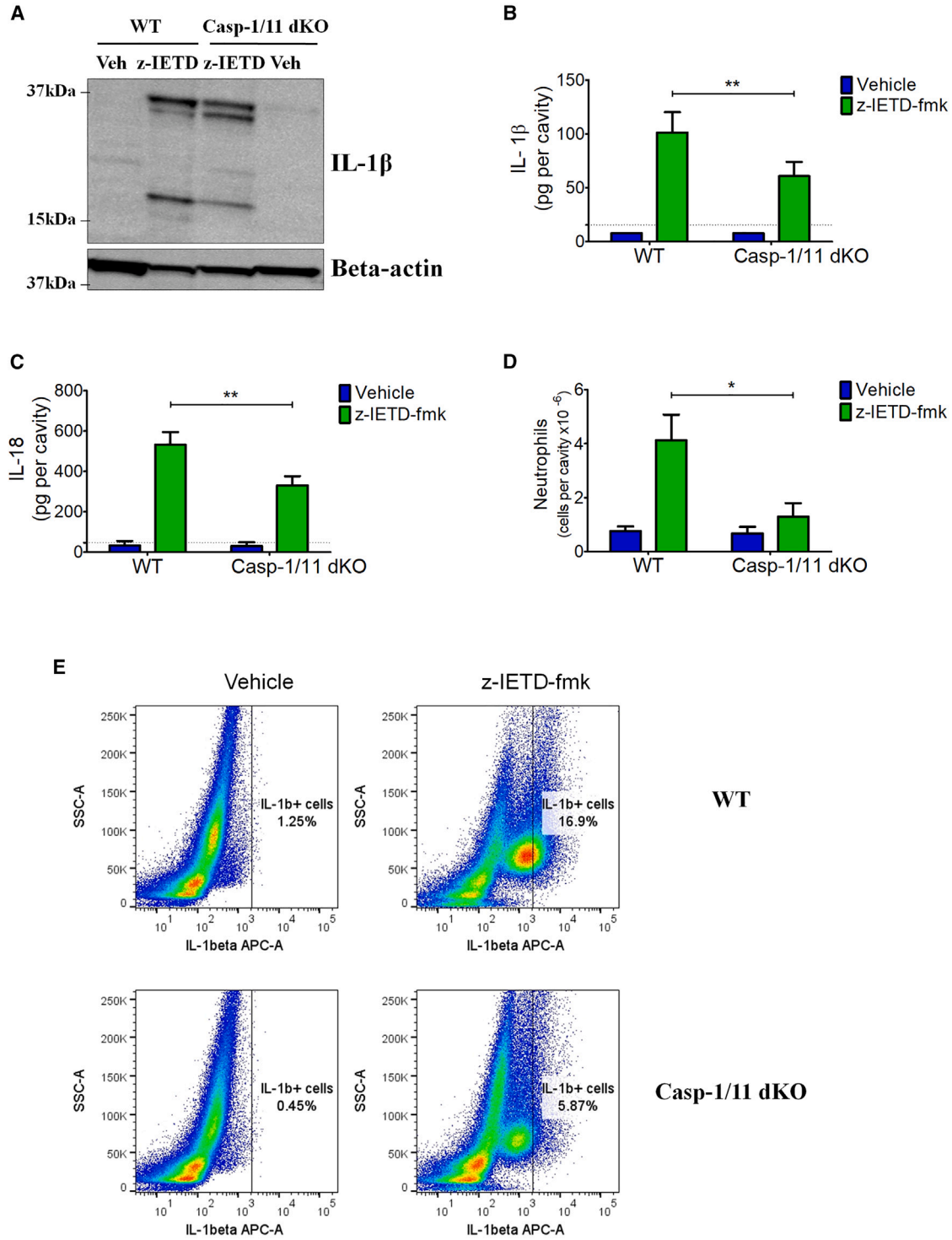

Figure 5. z-IETD-fmk-induced inflammation is partially dependent on caspase-1/-11

PLF samples were obtained from WT or *caspase-1/-11*$^{-/-}$ mice at 3 h after i.p. treatment with z-IETD-fmk or vehicle.

(A) IL-1β immunoblot of peritoneal cell lysates, with β-actin as a loading control. Shown is a blot representative of three separate experiments.

(B–E) IL-1β concentration (B), IL-18 concentration (C), neutrophil counts (D), and representative scatterplot (E) of IL-1β+ peritoneal cells after IL-1β intracellular staining.

(B–D) Mean + SDs of 5 duplicate measurements, each conducted on a different animal during one experiment. *$p < 0.05$; **$p < 0.01$, as determined by the Mann-Whitney U test.

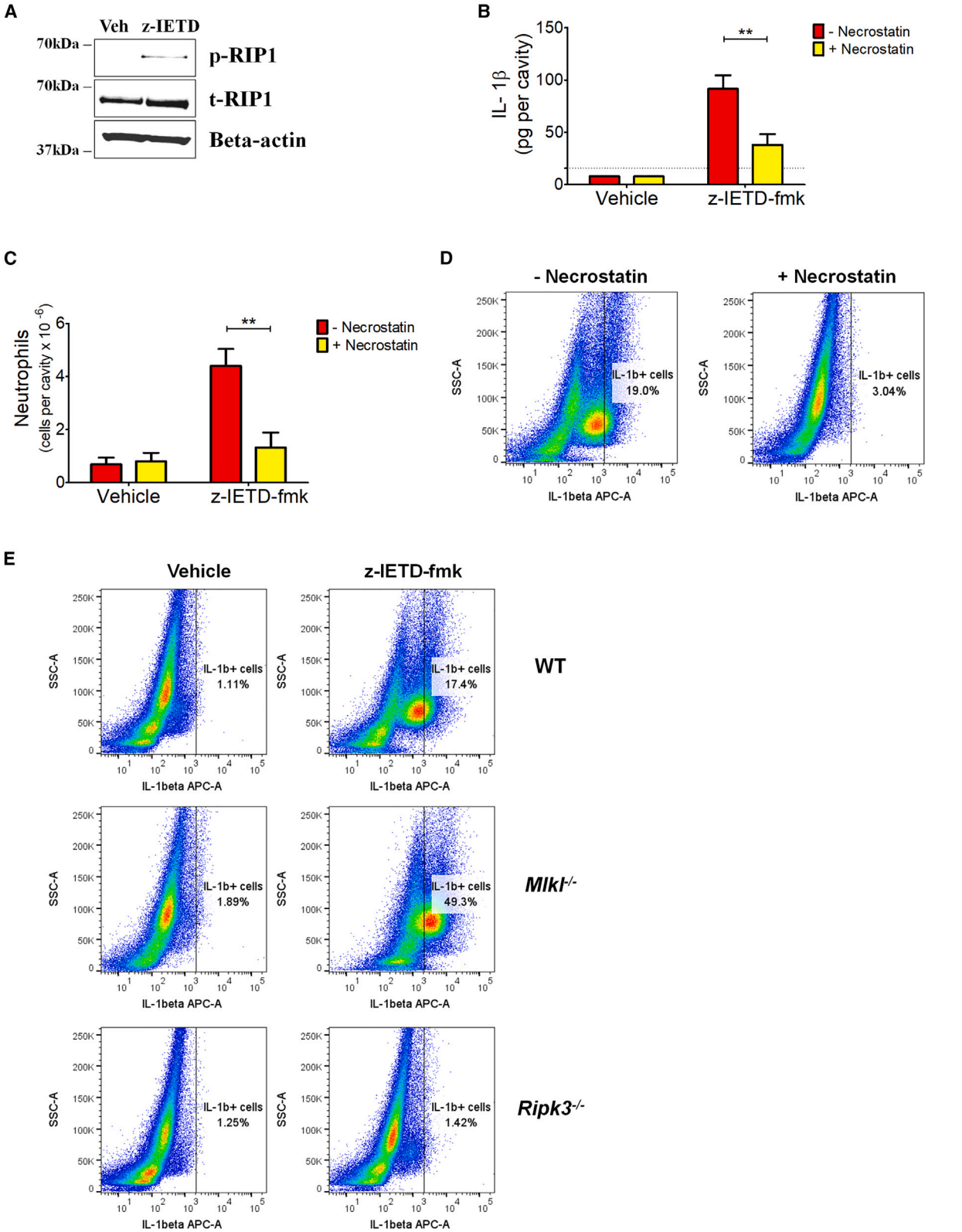

(legend on next page)

S7H). Notably, z-IETD-fmk treatment did not ameliorate lethality or increase circulating cytokine levels in mice lacking Casp1/11 or RIPK3, indicating that these molecules are required for the therapeutic effects of IETD (Figures S7C–S7H). Exogenous administration of recombinant IFN-β moderately ameliorated GBS-induced sepsis in wild-type mice, in general agreement with the notion that IFN-β promotes host defenses against GBS and other extracellular bacteria.[36] However, IFN-β treatment was ineffective in Casp1/11 or RIPK3 KO mice, indicating that these proteins are involved the therapeutic activities of the cytokine (Figure S7).

Excessive inflammatory reactions can be dangerous not only in the context of septic shock but also during pneumonia since the presence of exudate in the alveolar spaces can hinder gas exchange, resulting in respiratory insufficiency. Therefore, we assessed whether z-IETD-fmk might be detrimental for the outcome of pneumonia using a model of infection by *Streptococcus pneumoniae*, the main cause of community-acquired pneumonia worldwide.[37,38] Mice were challenged with 1×10^8 colony-forming units (CFUs) of the serotype 2D39 reference strain by the intranasal route and, after 24 h, were treated daily with z-IETD-fmk (6 mg/kg i.v.) or vehicle. Under these conditions, 62% of the mice receiving vehicle showed signs of irreversible disease and were humanely euthanized within 5 days, while only 12% of z-IETD-fmk-treated animals succumbed to infection ($p < 0.05$; Figure 7B). A significantly lower bacterial burden was detected in z-IETD-fmk-treated mice compared with control animals (Figure 7B). Moreover, z-IETD-fmk had similar protective activities in a model of pneumonia caused by carbapenem-resistant *Klebsiella pneumoniae* (Figure 7C). Collectively, our data indicate that z-IETD-fmk administration produces marked protective effects in models of septic shock or invasive pneumonia caused by partially or extremely antibiotic-resistant pathogens.

DISCUSSION

Unless suppressed by the catalytic activity of caspase-8, inflammatory changes occur by default in some epithelial and endothelial tissues, pointing to a unique homeostatic role of this enzyme among all proteases.[11,39,40] However, the mechanisms underlying this function are incompletely understood, and whether caspase-8 can play a homeostatic role in cells of the innate immune system is presently unclear. Data presented here suggest that caspase-8 suppresses a pro-inflammatory program that is spontaneously activated in neutrophils, depends on RIPK3 and is sustained by tonic IFN-β production. We found that exposure of bone marrow neutrophils to a caspase-8 inhibitor is sufficient to induce the production of pro-inflammatory cytokines at both the mRNA and protein level in the absence of other external stimuli. Moreover, i.p. injection of the inhibitor induced marked neutrophil recruitment and the appearance of a characteristic pattern of chemokines and cytokines known to be potentially released by neutrophils upon activation.[41] This distinctive cytokine signature included several members of the Cxcl chemokine family, CCL2, IL-17, TIMP-1, and IL-1β, while TNF-α/IL-12 responses were less pronounced. In addition, neutrophils were found to represent most of the IL-1β-producing cells and to be required for cytokine elevations in IETD-induced peritoneal exudates, as shown by, respectively, immunofluorescence and *in vivo* neutrophil depletion experiments.

Throughout our study, we used the caspase-8 inhibitor z-IETD-fmk, which was selected according to the reported substrate preferences for this enzyme.[42] However, like other tetrapeptide inhibitors, z-IETD-fmk can cross-inhibit other caspases due to overlap in the substrate preferences of these enzymes.[43,44] To provide maximal selectivity, z-IETD-fmk dosing was titrated here in comparison to other fmk-based inhibitors, such as the caspase-1 inhibitor z-YVAD-fmk and the pan-caspase inhibitor z-VAD-fmk. Under the conditions we used, the pro-inflammatory changes induced by z-IETD-fmk were due to specific caspase-8 inhibition since they were completely absent in animals lacking caspase-8. Moreover, these effects depended on the kinase activity of RIPK1 and on RIPK3, which are both substrates of caspase-8 but not of other caspases.[45,46]

Notably, although completely dependent on the presence of RIPK3, such mechanisms were independent from MLKL, the essential executioner of necroptosis, and occurred in the absence of other forms of cell death. Until recently, the presumption was that activation of the RIPK1/3 pathway invariably led to necroptosis and that this form of programmed cell death was entirely responsible for the inflammatory events unleashed by caspase-8 inhibition.[47] However, it has become increasingly clear that RIPK1/3 are involved in several inflammatory responses occurring in the absence of necroptosis or other forms of cell death.[30] For example, the kinase activities of both RIPK1 and -3 were required for activating an antiviral and pro-inflammatory transcriptional program that restricted infection by West Nile and Zika viruses in an MLKL- and cell death-independent fashion.[48,49] In a similar vein, in the absence of caspase-8, LPS engaged a RIPK1/3-dependent and MLKL-independent pathway in macrophages, leading to the production of pro-inflammatory cytokines.[50,51] In addition, RIPK3 was required for LPS-induced nuclear factor κB (NF-κB) activation and pro-inflammatory cytokine production in bone-marrow-derived dendritic cells.[52]

Figure 6. z-IETD-fmk-induced inflammation is dependent on RIPK1 activation and RIPK3 but not on MLKL

PLF samples were obtained at 3 h after treating mice with z-IETD-fmk (6 mg/kg i.p.) or vehicle.

(A) Representative immunoblot of peritoneal cell lysates using antibodies specific for phosphorylated or total RIPK1 (p-RIP1 or t-RIP1, respectively), with β-actin as a loading control.

(B–D) The effects of necrostatin-1 on z-IETD-fmk-induced inflammation were assessed by measuring IL-1β levels (B), neutrophil numbers (C), and intracellular staining for IL-1β (D) in PLF samples from mice pretreated i.p. with necrostatin (1.85 mg/kg body weight in 0.2 mL PBS) or PBS at 1 h before z-IETD-fmk administration. (B and C) Means + SDs of 5 duplicate measurements, each conducted on a different animal during one experiment. **$p < 0.01$, as determined by the Mann-Whitney U test.

(E) Scatterplots of IL-1β+ peritoneal cells obtained from WT, *Mlkl*$^{-/-}$, or *Ripk3*$^{-/-}$ mice at 3 h after administration of z-IETD-fmk (6 mg/kg i.p.) or vehicle. Data from one experiment of three showing similar results.

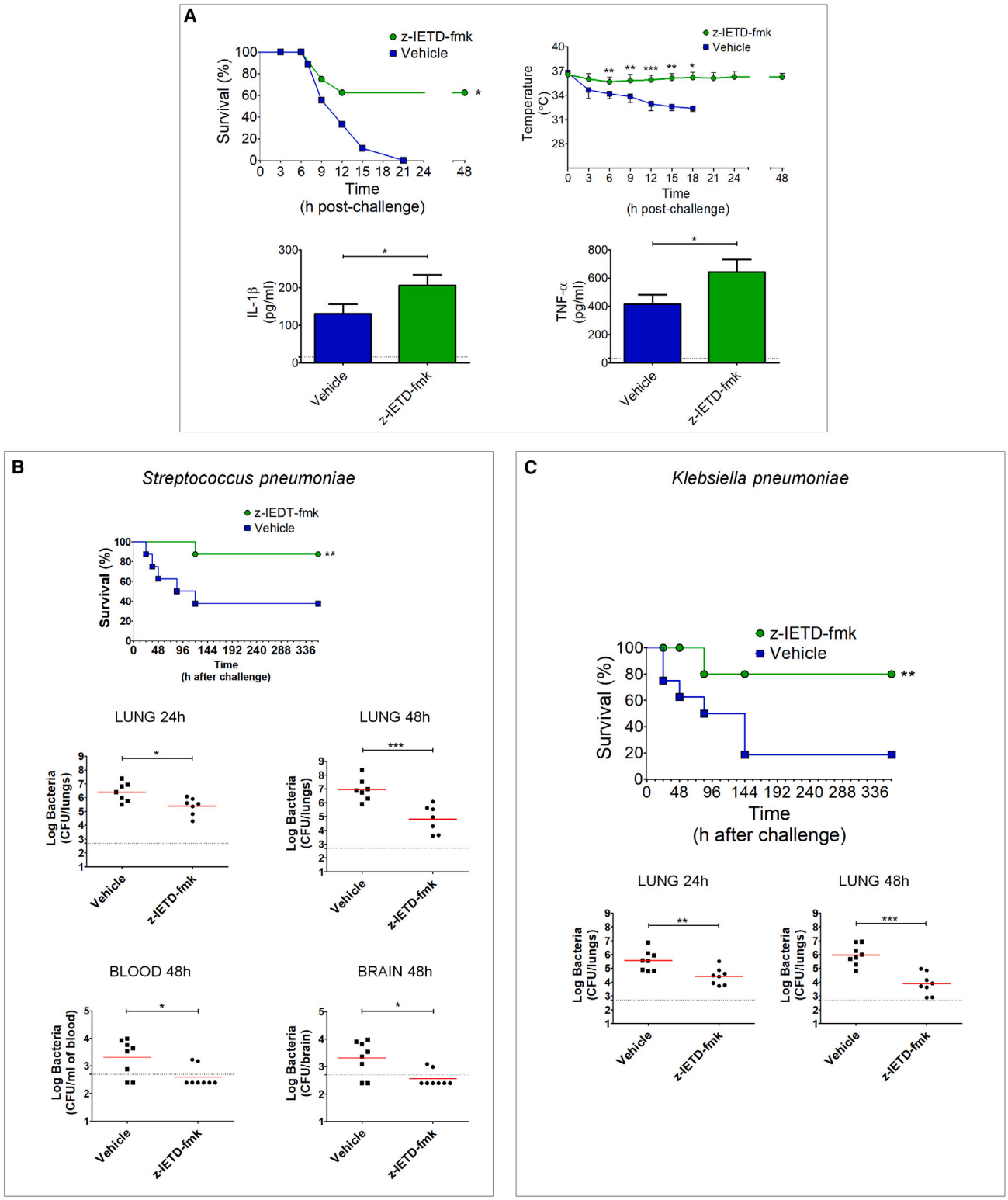

Figure 7. z-IETD-fmk alleviates LPS-induced shock and bacterial pneumonia

(A) C57BL/6 mice were pretreated i.v. with z-IETD-fmk (6 mg/kg) or vehicle at 1 h before challenge with LPS (40 mg/kg). Mice were kept under observation and humanely euthanized when showing clinical signs of irreversible shock (top left). Rectal temperature (top right) was measured every 3 h post-challenge. IL-1β and

(legend continued on next page)

Of note, the RIPK3-dependent pro-inflammatory program we describe in neutrophils requires the presence of IFN-β. Clearly, other stimuli, in addition to IFN-β, might be responsible for constitutive RIPK3-dependent gene activation. Various receptor families, including death receptors, TLRs, and cytosolic nucleic acid sensors, can trigger RIPK1/3 and caspase-8 activation upon binding to their cognate ligands.[30] Notably, during their maturation in the bone marrow and in peripheral blood, neutrophils activate a series of genes encoding for death receptor-ligand pairs such as TNF-TNFR1, TRAIL-TRAILR2, and TNFRSF12A-TWEAK,[23] raising the possibility that autocrine loops involving one or more death receptors drive tonic caspase-8 and RIPK3 activation. We also found in the present study that caspase-1/-11 are at least partially responsible for the inflammatory changes triggered by caspase-8 inhibition. However, the mechanism involved did not require NALP3, a component of the caspase-1 inflammasome that can be activated by RIPK3 in macrophages in the absence of caspase-8.[53,54] Recently, the expression of catalytically inactive caspase-8 in intestinal epithelial cells was found to provide a nucleation signal for the formation of a caspase-1 inflammasome,[19,55] and a similar function of the caspase-8 scaffold might be operating in our IETD-treated neutrophils.

Permanent deletion or inactivation of caspase 8 can produce detrimental effects due to severe necroptosis or pyroptosis,[19,53] which may be exacerbated by the presence of bacterial TLR agonists.[56] However, temporary inhibition of caspase-8 had no obvious detrimental effects in the present study and ameliorated the outcome of lethal infections due to augmented neutrophil-mediated bacterial clearance. Indeed, in the infection models we used, host-protective neutrophil influx is triggered by Cxcl1 and Cxcl2 and sustained by neutrophil-derived Cxcl2 and IL-1β production[57–59] in a sequence that could be recapitulated here by caspase-8 inhibition even in the absence of bacterial stimulation.

Notably, the ability of caspase-8 inhibition to prevent lethality in our sepsis models could be explained not only by increased host defenses but also by attenuation of the indirect toxic effects of bacterial TLR agonists. Indeed, treatment with z-IETD-fmk prevented here lethality in mice challenged with high-dose endotoxin, in agreement with the well-established, essential role of caspase-8 in driving lethality and apoptotic damage during sepsis.[60] Historically, therapeutic approaches aimed at augmenting host defenses against infection by cytokine administration or potentiation of endogenous cytokine production have been met with the risk of inducing harmful inflammatory reactions and shock.[61] Strategies involving selective caspase-8 inhibition, as proposed here, seem attractive because they have the potential to augment the production of pro-inflammatory cytokines while, at the same time, protecting against their toxic effects, including cell death. Therefore, it appears that the pro-inflammatory program described here can be harnessed against difficult-to-treat bacterial diseases, such as those caused by antibiotic-resistant pathogens.

It was recently reported that the pan-caspase inhibitor quinoline-valine-aspartic acid-difluorophenoxymethyl ketone (Q-VD-OPH) has therapeutic effects against dermatitis caused by *Staphylococcus aureus* and other bacteria by reducing the size of dermonecrotic lesions and bacterial burden in the skin.[62] Whether this or other pan-caspase inhibitors are effective in infections involving organs other than the skin or in systemic infections has not been reported and, in our hands, the pan-caspase inhibitor z-VAD-fmk was ineffective against bacterial peritonitis. The pan-caspase inhibition approach described in the study cited above[62] differs from the caspase-8-selective approach proposed here in another important aspect. In that study, the beneficial effects of Q-VD-OPH were linked to inhibition of phagocyte apoptosis and were independent from caspase-1/-11. In contrast, the ability of z-IETD-fmk to promote bacterial clearance was independent here from effects on cell death and depended instead on the presence of caspase-1/-11. Moreover, this caspase-1/-11 requirement accounted for the inability of the pan-caspase inhibitor z-VAD-fmk at promoting antibacterial defenses like those triggered by z-IETD-fmk, despite the ability of both compounds to inhibit caspase-8. In general, caspase-1 inhibition should be considered with caution in systemic infections, based on the essential role of caspase-1 in host defenses against many pathogens.[63] Accordingly, our data underscore the importance of selectively targeting caspase-8 in anti-infectious strategies aiming at potentiating host defenses.

Limitations of the study

Evidence for the effectiveness of selective caspase-8 inhibition in the immunotherapy of bacterial diseases was obtained here using mouse infection models. Therapeutic use of caspase-8 inhibition in humans will require confirmation in larger animal models as well as the development of more selective and less toxic drugs than those currently available. Moreover, the safety of caspase-8 inhibitors should be carefully assessed since caspase-8 deficiency in humans is associated with defects in lymphocyte activation and immunodeficiency.[10] Another limitation of the present study is that the mechanisms underlying the caspase-1/-11 requirement for the protective effects of caspase-8 inhibition have been incompletely identified. Future studies will be needed to ascertain whether such mechanisms predominantly involve inflammasome activation or enhanced transcription of pro-inflammatory genes. Finally, although this study shows that neutrophils are major cytokine producers in response to caspase-8 inhibition, the involvement of other cell types cannot be excluded. Notably, macrophages represented a sizable proportion of the IL-1β-producing cells after *in vivo* stimulation with a caspase-8 inhibitor, although

TNF-α concentrations were measured in blood samples obtained at 2 h after challenge (bottom). Shown are cumulative data from two experiments, each involving 4 animals per group.
(B) Mice were treated with z-IETD-fmk (6 mg/kg, i.v.) or vehicle at 24, 48, 72, 96, and 120 h after intranasal challenge with *S. pneumoniae* (1×10^8 CFU/mouse).
(C) Mice were treated with z-IETD-fmk (6 mg/kg, i.v.) or vehicle at 24, 48, 72, 96, and 120 h after intranasal challenge with *K. pneumoniae* (5×10^7 CFU/mouse).
(B and C) The top panels show survival curves obtained by cumulating data from two experiments, each involving 8 animals per group. The bottom panels show log CFUs in organs obtained at 24 or 48 h after challenge. *$p < 0.05$; **$p < 0.01$; ***$p < 0.001$, versus vehicle-treated mice, as determined by Kaplan-Meier analysis (survival) or by the Mann-Whitney U test (temperature, cytokine concentrations, and log CFUs).

these cells did not produce IL-1β- and neutrophil-attracting chemokines when stimulated *in vitro*. Moreover, we focused here on inflammatory peritoneal cells and did not examine cytokine production in other body districts. Future studies will examine various cell types for their *in vivo* and *in vitro* responses to IETD treatment by global gene expression analysis. In view of the strict IFN-β requirement for IETD responses, we will focus on the identification of IFN-β-producing cell types.

STAR★METHODS

Detailed methods are provided in the online version of this paper and include the following:

- KEY RESOURCES TABLE
- RESOURCE AVAILABILITY
  - Lead contact
  - Materials availability
  - Data and code availability
- EXPERIMENTAL MODEL AND SUBJECT DETAILS
  - Mice
  - Human blood samples
  - Bacterial strains
- METHOD DETAILS
  - Administration of caspase inhibitors
  - Mouse infections and septic shock models
  - *In vitro* cell stimulation
  - Cytokine determinations
  - Western blot analysis
  - Immuno-staining and flow cytometric analysis
- QUANTIFICATION AND STATISTICAL ANALYSIS

SUPPLEMENTAL INFORMATION

Supplemental information can be found online at https://doi.org/10.1016/j.xcrm.2023.101098.

ACKNOWLEDGMENTS

We thank Andrea Cappello for helpful discussions and technical help. We also thank Cameron Choquette for assistance in providing mouse models. This study was supported by research funding to C.B. (grant 3/2020) from Scylla Biotech Srl, a spin-off company of the University of Messina. The study was also supported in part by funding from the National Institutes of Health to E.L. (NIH grant R01AI146855) and by grant 223255/F50 from the Research Council of Norway through its Centers of Excellence funding scheme. Support from the above organizations did not include publication expenses, which were entirely sustained by the University of Messina through the APC initiative.

AUTHOR CONTRIBUTIONS

G.L., A.F., C.B., and G.T. conceived the study. G.L. and A.F. performed most experiments. G.V.D.G., F.C., L.R., and A.K.M. performed other experiments. E.L. provided crucial models and advice. T.E. provided crucial advice and data obtained with human leukocyte analysis. G.L., C.B., and G.T. wrote the paper.

DECLARATION OF INTERESTS

G.T. is an employee and C.B. is the founder and owner of Scylla Biotech Srl, a company that filed a patent application (UIBM 102023000000834) partially based on this study. G.V.D.V. has been recently employed by Scylla Biotech.

Received: February 18, 2023
Revised: May 7, 2023
Accepted: June 8, 2023
Published: June 29, 2023

REFERENCES

1. Van Opdenbosch, N., and Lamkanfi, M. (2019). Caspases in cell death, inflammation, and disease. Immunity *50*, 1352–1364. https://doi.org/10.1016/j.immuni.2019.05.020.
2. Julien, O., and Wells, J.A. (2017). Caspases and their substrates. Cell Death Differ. *24*, 1380–1389. https://doi.org/10.1038/cdd.2017.44.
3. Orning, P., and Lien, E. (2021). Multiple roles of caspase-8 in cell death, inflammation, and innate immunity. J. Leukoc. Biol. *109*, 121–141. https://doi.org/10.1002/JLB.3MR0420-305R.
4. Tummers, B., and Green, D.R. (2017). Caspase-8: regulating life and death. Immunol. Rev. *277*, 76–89. https://doi.org/10.1111/imr.12541.
5. Newton, K., Dixit, V.M., and Kayagaki, N. (2021). Dying cells fan the flames of inflammation. Science *374*, 1076–1080. https://doi.org/10.1126/science.abi5934.
6. Orning, P., Weng, D., Starheim, K., Ratner, D., Best, Z., Lee, B., Brooks, A., Xia, S., Wu, H., Kelliher, M.A., et al. (2018). Pathogen blockade of TAK1 triggers caspase-8-dependent cleavage of gasdermin D and cell death. Science *362*, 1064–1069. https://doi.org/10.1126/science.aau2818.
7. Shi, J., Gao, W., and Shao, F. (2017). Pyroptosis: gasdermin-mediated programmed necrotic cell death. Trends Biochem. Sci. *42*, 245–254. https://doi.org/10.1016/j.tibs.2016.10.004.
8. Newton, K., Wickliffe, K.E., Dugger, D.L., Maltzman, A., Roose-Girma, M., Dohse, M., Kőműves, L., Webster, J.D., and Dixit, V.M. (2019). Cleavage of RIPK1 by caspase-8 is crucial for limiting apoptosis and necroptosis. Nature *574*, 428–431. https://doi.org/10.1038/s41586-019-1548-x.
9. Oberst, A., Dillon, C.P., Weinlich, R., McCormick, L.L., Fitzgerald, P., Pop, C., Hakem, R., Salvesen, G.S., and Green, D.R. (2011). Catalytic activity of the caspase-8-FLIP(L) complex inhibits RIPK3-dependent necrosis. Nature *471*, 363–367. https://doi.org/10.1038/nature09852.
10. Chun, H.J., Zheng, L., Ahmad, M., Wang, J., Speirs, C.K., Siegel, R.M., Dale, J.K., Puck, J., Davis, J., Hall, C.G., et al. (2002). Pleiotropic defects in lymphocyte activation caused by caspase-8 mutations lead to human immunodeficiency. Nature *419*, 395–399. https://doi.org/10.1038/nature01063.
11. Lehle, A.S., Farin, H.F., Marquardt, B., Michels, B.E., Magg, T., Li, Y., Liu, Y., Ghalandary, M., Lammens, K., Hollizeck, S., et al. (2019). Intestinal inflammation and dysregulated immunity in patients with inherited caspase-8 deficiency. Gastroenterology *156*, 275–278. https://doi.org/10.1053/j.gastro.2018.09.041.
12. Allam, R., Lawlor, K.E., Yu, E.C.W., Mildenhall, A.L., Moujalled, D.M., Lewis, R.S., Ke, F., Mason, K.D., White, M.J., Stacey, K.J., et al. (2014). Mitochondrial apoptosis is dispensable for NLRP3 inflammasome activation but non-apoptotic caspase-8 is required for inflammasome priming. EMBO Rep. *15*, 982–990. https://doi.org/10.15252/embr.201438463.
13. DeLaney, A.A., Berry, C.T., Christian, D.A., Hart, A., Bjanes, E., Wynosky-Dolfi, M.A., Li, X., Tummers, B., Udalova, I.A., Chen, Y.H., et al. (2019). Caspase-8 promotes c-Rel-dependent inflammatory cytokine expression and resistance against Toxoplasma gondii. Proc. Natl. Acad. Sci. USA *116*, 11926–11935. https://doi.org/10.1073/pnas.1820529116.
14. Ganesan, S., Rathinam, V.A.K., Bossaller, L., Army, K., Kaiser, W.J., Mocarski, E.S., Dillon, C.P., Green, D.R., Mayadas, T.N., Levitz, S.M., et al. (2014). Caspase-8 modulates dectin-1 and complement receptor 3-driven IL-1beta production in response to beta-glucans and the fungal pathogen, Candida albicans. J. Immunol. *193*, 2519–2530. https://doi.org/10.4049/jimmunol.1400276.
15. Gurung, P., Anand, P.K., Malireddi, R.K.S., Vande Walle, L., Van Opdenbosch, N., Dillon, C.P., Weinlich, R., Green, D.R., Lamkanfi, M., and Kanneganti, T.D. (2014). FADD and caspase-8 mediate priming and activation

of the canonical and noncanonical Nlrp3 inflammasomes. J. Immunol. *192*, 1835–1846. https://doi.org/10.4049/jimmunol.1302839.

16. Man, S.M., Tourlomousis, P., Hopkins, L., Monie, T.P., Fitzgerald, K.A., and Bryant, C.E. (2013). Salmonella infection induces recruitment of Caspase-8 to the inflammasome to modulate IL-1beta production. J. Immunol. *191*, 5239–5246. https://doi.org/10.4049/jimmunol.1301581.
17. Philip, N.H., DeLaney, A., Peterson, L.W., Santos-Marrero, M., Grier, J.T., Sun, Y., Wynosky-Dolfi, M.A., Zwack, E.E., Hu, B., Olsen, T.M., et al. (2016). Activity of uncleaved caspase-8 controls anti-bacterial immune defense and TLR-induced cytokine production independent of cell death. PLoS Pathog. *12*, e1005910. https://doi.org/10.1371/journal.ppat.1005910.
18. Weng, D., Marty-Roix, R., Ganesan, S., Proulx, M.K., Vladimer, G.I., Kaiser, W.J., Mocarski, E.S., Pouliot, K., Chan, F.K.M., Kelliher, M.A., et al. (2014). Caspase-8 and RIP kinases regulate bacteria-induced innate immune responses and cell death. Proc. Natl. Acad. Sci. USA *111*, 7391–7396. https://doi.org/10.1073/pnas.1403477111.
19. Fritsch, M., Günther, S.D., Schwarzer, R., Albert, M.C., Schorn, F., Werthenbach, J.P., Schiffmann, L.M., Stair, N., Stocks, H., Seeger, J.M., et al. (2019). Caspase-8 is the molecular switch for apoptosis, necroptosis and pyroptosis. Nature *575*, 683–687. https://doi.org/10.1038/s41586-019-1770-6.
20. Holmes, A.H., Moore, L.S.P., Sundsfjord, A., Steinbakk, M., Regmi, S., Karkey, A., Guerin, P.J., and Piddock, L.J.V. (2016). Understanding the mechanisms and drivers of antimicrobial resistance. Lancet *387*, 176–187. https://doi.org/10.1016/S0140-6736(15)00473-0.
21. Lentini, G., De Gaetano, G.V., Famà, A., Galbo, R., Coppolino, F., Mancuso, G., Teti, G., and Beninati, C. (2022). Neutrophils discriminate live from dead bacteria by integrating signals initiated by Fprs and TLRs. EMBO J. *41*, e109386. https://doi.org/10.15252/embj.2021109386.
22. Ley, K., Hoffman, H.M., Kubes, P., Cassatella, M.A., Zychlinsky, A., Hedrick, C.C., and Catz, S.D. (2018). Neutrophils: new insights and open questions. Sci. Immunol. *3*, eaat4579. https://doi.org/10.1126/sciimmunol.aat4579.
23. Theilgaard-Mönch, K., Jacobsen, L.C., Borup, R., Rasmussen, T., Bjerregaard, M.D., Nielsen, F.C., Cowland, J.B., and Borregaard, N. (2005). The transcriptional program of terminal granulocytic differentiation. Blood *105*, 1785–1796. https://doi.org/10.1182/blood-2004-08-3346.
24. Grieshaber-Bouyer, R., Radtke, F.A., Cunin, P., Stifano, G., Levescot, A., Vijaykumar, B., Nelson-Maney, N., Blaustein, R.B., Monach, P.A., and Nigrovic, P.A.; ImmGen Consortium (2021). The neutrotime transcriptional signature defines a single continuum of neutrophils across biological compartments. Nat. Commun. *12*, 2856. https://doi.org/10.1038/s41467-021-22973-9.
25. Landwehr-Kenzel, S., and Henneke, P. (2014). Interaction of Streptococcus agalactiae and cellular innate immunity in colonization and disease. Front. Immunol. *5*, 519. https://doi.org/10.3389/fimmu.2014.00519.
26. Mancuso, G., Gambuzza, M., Midiri, A., Biondo, C., Papasergi, S., Akira, S., Teti, G., and Beninati, C. (2009). Bacterial recognition by TLR7 in the lysosomes of conventional dendritic cells. Nat. Immunol. *10*, 587–594. https://doi.org/10.1038/ni.1733.
27. Mancuso, G., Midiri, A., Beninati, C., Biondo, C., Galbo, R., Akira, S., Henneke, P., Golenbock, D., and Teti, G. (2004). Dual role of TLR2 and myeloid differentiation factor 88 in a mouse model of invasive group B streptococcal disease. J. Immunol. *172*, 6324–6329. https://doi.org/10.4049/jimmunol.172.10.6324.
28. Teti, G., Mancuso, G., and Tomasello, F. (1993). Cytokine appearance and effects of anti-tumor necrosis factor alpha antibodies in a neonatal rat model of group B streptococcal infection. Infect. Immun. *61*, 227–235. https://doi.org/10.1128/iai.61.1.227-235.1993.
29. Poreba, M., Strózyk, A., Salvesen, G.S., and Drag, M. (2013). Caspase substrates and inhibitors. Cold Spring Harb. Perspect. Biol. *5*, a008680. https://doi.org/10.1101/cshperspect.a008680.
30. Newton, K. (2020). Multitasking kinase RIPK1 regulates cell death and inflammation. Cold Spring Harb. Perspect. Biol. *12*, a036368. https://doi.org/10.1101/cshperspect.a036368.
31. Pham, C.T.N. (2008). Neutrophil serine proteases fine-tune the inflammatory response. Int. J. Biochem. Cell Biol. *40*, 1317–1333. https://doi.org/10.1016/j.biocel.2007.11.008.
32. Biondo, C., Lentini, G., Beninati, C., and Teti, G. (2019). The dual role of innate immunity during influenza. Biomed. J. *42*, 8–18. https://doi.org/10.1016/j.bj.2018.12.009.
33. Patel, S., Webster, J.D., Varfolomeev, E., Kwon, Y.C., Cheng, J.H., Zhang, J., Dugger, D.L., Wickliffe, K.E., Maltzman, A., Sujatha-Bhaskar, S., et al. (2020). RIP1 inhibition blocks inflammatory diseases but not tumor growth or metastases. Cell Death Differ. *27*, 161–175. https://doi.org/10.1038/s41418-019-0347-0.
34. Signorino, G., Mohammadi, N., Patanè, F., Buscetta, M., Venza, M., Venza, I., Mancuso, G., Midiri, A., Alexopoulou, L., Teti, G., et al. (2014). Role of Toll-like receptor 13 in innate immune recognition of group B streptococci. Infect. Immun. *82*, 5013–5022. https://doi.org/10.1128/IAI.02282-14.
35. Teti, G., Mancuso, G., Losi, E., Tomasello, F., Cusumano, V., Gambuzza, M., and Petrelli, M.L. (1997). Age-related sensitivity of neonatal mice to toxicity induced by heat-killed group B streptococci. Adv. Exp. Med. Biol. *418*, 945–947. https://doi.org/10.1007/978-1-4899-1825-3_222.
36. Mancuso, G., Midiri, A., Biondo, C., Beninati, C., Zummo, S., Galbo, R., Tomasello, F., Gambuzza, M., Macrì, G., Ruggeri, A., et al. (2007). Type I IFN signaling is crucial for host resistance against different species of pathogenic bacteria. J. Immunol. *178*, 3126–3133. https://doi.org/10.4049/jimmunol.178.5.3126.
37. Watson, D.A., Musher, D.M., Jacobson, J.W., and Verhoef, J. (1993). A brief history of the pneumococcus in biomedical research: a panoply of scientific discovery. Clin. Infect. Dis. *17*, 913–924. https://doi.org/10.1093/clinids/17.5.913.
38. Famà, A., Midiri, A., Mancuso, G., Biondo, C., Lentini, G., Galbo, R., Giardina, M.M., De Gaetano, G.V., Romeo, L., Teti, G., and Beninati, C. (2020). Nucleic acid-sensing toll-like receptors play a dominant role in innate immune recognition of pneumococci. mBio *11*, e00415-20. https://doi.org/10.1128/mBio.00415-20.
39. Kovalenko, A., Kim, J.C., Kang, T.B., Rajput, A., Bogdanov, K., Dittrich-Breiholz, O., Kracht, M., Brenner, O., and Wallach, D. (2009). Caspase-8 deficiency in epidermal keratinocytes triggers an inflammatory skin disease. J. Exp. Med. *206*, 2161–2177. https://doi.org/10.1084/jem.20090616.
40. Yuan, J., Najafov, A., and Py, B.F. (2016). Roles of caspases in necrotic cell death. Cell *167*, 1693–1704. https://doi.org/10.1016/j.cell.2016.11.047.
41. Tecchio, C., Micheletti, A., and Cassatella, M.A. (2014). Neutrophil-derived cytokines: facts beyond expression. Front. Immunol. *5*, 508. https://doi.org/10.3389/fimmu.2014.00508.
42. Thornberry, N.A., Rano, T.A., Peterson, E.P., Rasper, D.M., Timkey, T., Garcia-Calvo, M., Houtzager, V.M., Nordstrom, P.A., Roy, S., Vaillancourt, J.P., et al. (1997). A combinatorial approach defines specificities of members of the caspase family and granzyme B. Functional relationships established for key mediators of apoptosis. J. Biol. Chem. *272*, 17907–17911. https://doi.org/10.1074/jbc.272.29.17907.
43. Pereira, N.A., and Song, Z. (2008). Some commonly used caspase substrates and inhibitors lack the specificity required to monitor individual caspase activity. Biochem. Biophys. Res. Commun. *377*, 873–877. https://doi.org/10.1016/j.bbrc.2008.10.101.
44. Poreba, M., Groborz, K., Navarro, M., Snipas, S.J., Drag, M., and Salvesen, G.S. (2019). Caspase selective reagents for diagnosing apoptotic mechanisms. Cell Death Differ. *26*, 229–244. https://doi.org/10.1038/s41418-018-0110-y.
45. Feng, S., Yang, Y., Mei, Y., Ma, L., Zhu, D.E., Hoti, N., Castanares, M., and Wu, M. (2007). Cleavage of RIP3 inactivates its caspase-independent

apoptosis pathway by removal of kinase domain. Cell. Signal. *19*, 2056–2067. https://doi.org/10.1016/j.cellsig.2007.05.016.

46. Lin, Y., Devin, A., Rodriguez, Y., and Liu, Z.G. (1999). Cleavage of the death domain kinase RIP by caspase-8 prompts TNF-induced apoptosis. Genes Dev. *13*, 2514–2526. https://doi.org/10.1101/gad.13.19.2514.
47. Pasparakis, M., and Vandenabeele, P. (2015). Necroptosis and its role in inflammation. Nature *517*, 311–320. https://doi.org/10.1038/nature14191.
48. Daniels, B.P., Kofman, S.B., Smith, J.R., Norris, G.T., Snyder, A.G., Kolb, J.P., Gao, X., Locasale, J.W., Martinez, J., Gale, M., Jr., et al. (2019). The nucleotide sensor ZBP1 and kinase RIPK3 induce the enzyme IRG1 to promote an antiviral metabolic state in neurons. Immunity *50*, 64–76.e4. https://doi.org/10.1016/j.immuni.2018.11.017.
49. Daniels, B.P., Snyder, A.G., Olsen, T.M., Orozco, S., Oguin, T.H., 3rd, Tait, S.W.G., Martinez, J., Gale, M., Jr., Loo, Y.M., and Oberst, A. (2017). RIPK3 restricts viral pathogenesis via cell death-independent neuroinflammation. Cell *169*, 301–313.e11. https://doi.org/10.1016/j.cell.2017.03.011.
50. Najjar, M., Saleh, D., Zelic, M., Nogusa, S., Shah, S., Tai, A., Finger, J.N., Polykratis, A., Gough, P.J., Bertin, J., et al. (2016). RIPK1 and RIPK3 kinases promote cell-death-independent inflammation by toll-like receptor 4. Immunity *45*, 46–59. https://doi.org/10.1016/j.immuni.2016.06.007.
51. Saleh, D., Najjar, M., Zelic, M., Shah, S., Nogusa, S., Polykratis, A., Paczosa, M.K., Gough, P.J., Bertin, J., Whalen, M., et al. (2017). Kinase activities of RIPK1 and RIPK3 can direct IFN-beta synthesis induced by lipopolysaccharide. J. Immunol. *198*, 4435–4447. https://doi.org/10.4049/jimmunol.1601717.
52. Moriwaki, K., Balaji, S., McQuade, T., Malhotra, N., Kang, J., and Chan, F.K.M. (2014). The necroptosis adaptor RIPK3 promotes injury-induced cytokine expression and tissue repair. Immunity *41*, 567–578. https://doi.org/10.1016/j.immuni.2014.09.016.
53. Kang, T.B., Yang, S.H., Toth, B., Kovalenko, A., and Wallach, D. (2013). Caspase-8 blocks kinase RIPK3-mediated activation of the NLRP3 inflammasome. Immunity *38*, 27–40. https://doi.org/10.1016/j.immuni.2012.09.015.
54. Moriwaki, K., and Chan, F.K.M. (2016). Necroptosis-independent signaling by the RIP kinases in inflammation. Cell. Mol. Life Sci. *73*, 2325–2334. https://doi.org/10.1007/s00018-016-2203-4.
55. Newton, K., Wickliffe, K.E., Maltzman, A., Dugger, D.L., Reja, R., Zhang, Y., Roose-Girma, M., Modrusan, Z., Sagolla, M.S., Webster, J.D., and Dixit, V.M. (2019). Activity of caspase-8 determines plasticity between cell death pathways. Nature *575*, 679–682. https://doi.org/10.1038/s41586-019-1752-8.
56. Günther, C., Buchen, B., He, G.W., Hornef, M., Torow, N., Neumann, H., Wittkopf, N., Martini, E., Basic, M., Bleich, A., et al. (2015). Caspase-8 controls the gut response to microbial challenges by Tnf-alpha-dependent and independent pathways. Gut *64*, 601–610. https://doi.org/10.1136/gutjnl-2014-307226.
57. Biondo, C., Mancuso, G., Midiri, A., Signorino, G., Domina, M., Lanza Cariccio, V., Mohammadi, N., Venza, M., Venza, I., Teti, G., and Beninati, C. (2014). The interleukin-1beta/CXCL1/2/neutrophil axis mediates host protection against group B streptococcal infection. Infect. Immun. *82*, 4508–4517. https://doi.org/10.1128/IAI.02104-14.
58. Lentini, G., Famà, A., Biondo, C., Mohammadi, N., Galbo, R., Mancuso, G., Iannello, D., Zummo, S., Giardina, M., De Gaetano, G.V., et al. (2020). Neutrophils enhance their own influx to sites of bacterial infection via endosomal TLR-dependent Cxcl2 production. J. Immunol. *204*, 660–670. https://doi.org/10.4049/jimmunol.1901039.
59. Mohammadi, N., Midiri, A., Mancuso, G., Patanè, F., Venza, M., Venza, I., Passantino, A., Galbo, R., Teti, G., Beninati, C., and Biondo, C. (2016). Neutrophils directly recognize group B streptococci and contribute to interleukin-1beta production during infection. PLoS One *11*, e0160249. https://doi.org/10.1371/journal.pone.0160249.
60. Mandal, P., Feng, Y., Lyons, J.D., Berger, S.B., Otani, S., DeLaney, A., Tharp, G.K., Maner-Smith, K., Burd, E.M., Schaeffer, M., et al. (2018). Caspase-8 collaborates with caspase-11 to drive tissue damage and execution of endotoxic shock. Immunity *49*, 42–55.e6. https://doi.org/10.1016/j.immuni.2018.06.011.
61. Wallis, R.S., O'Garra, A., Sher, A., and Wack, A. (2022). Host-directed immunotherapy of viral and bacterial infections: past, present and future. Nat. Rev. Immunol. *23*, 121–133. https://doi.org/10.1038/s41577-022-00734-z.
62. Alphonse, M.P., Rubens, J.H., Ortines, R.V., Orlando, N.A., Patel, A.M., Dikeman, D., Wang, Y., Vuong, I., Joyce, D.P., Zhang, J., et al. (2021). Pan-caspase inhibition as a potential host-directed immunotherapy against MRSA and other bacterial skin infections. Sci. Transl. Med. *13*, eabe9887. https://doi.org/10.1126/scitranslmed.abe9887.
63. Man, S.M., Karki, R., and Kanneganti, T.D. (2017). Molecular mechanisms and functions of pyroptosis, inflammatory caspases and inflammasomes in infectious diseases. Immunol. Rev. *277*, 61–75. https://doi.org/10.1111/imr.12534.
64. Li, P., Allen, H., Banerjee, S., Franklin, S., Herzog, L., Johnston, C., McDowell, J., Paskind, M., Rodman, L., Salfeld, J., et al. (1995). Mice deficient in IL-1 beta-converting enzyme are defective in production of mature IL-1 beta and resistant to endotoxic shock. Cell *80*, 401–411. https://doi.org/10.1016/0092-8674(95)90490-5.
65. Newton, K., Sun, X., and Dixit, V.M. (2004). Kinase RIP3 is dispensable for normal NF-kappa Bs, signaling by the B-cell and T-cell receptors, tumor necrosis factor receptor 1, and Toll-like receptors 2 and 4. Mol. Cell Biol. *24*, 1464–1469. https://doi.org/10.1128/MCB.24.4.1464-1469.2004.
66. Murphy, J.M., Czabotar, P.E., Hildebrand, J.M., Lucet, I.S., Zhang, J.G., Alvarez-Diaz, S., Lewis, R., Lalaoui, N., Metcalf, D., Webb, A.I., et al. (2013). The pseudokinase MLKL mediates necroptosis via a molecular switch mechanism. Immunity *39*, 443–453. https://doi.org/10.1016/j.immuni.2013.06.018.
67. Erlandsson, L., Blumenthal, R., Eloranta, M.L., Engel, H., Alm, G., Weiss, S., and Leanderson, T. (1998). Interferon-beta is required for interferon-alpha production in mouse fibroblasts. Curr. Biol. *8*, 223–226. https://doi.org/10.1016/s0960-9822(98)70086-7.
68. Salmena, L., Lemmers, B., Hakem, A., Matysiak-Zablocki, E., Murakami, K., Au, P.Y.B., Berry, D.M., Tamblyn, L., Shehabeldin, A., Migon, E., et al. (2003). Essential role for caspase 8 in T-cell homeostasis and T-cell-mediated immunity. Genes Dev. *17*, 883–895. https://doi.org/10.1101/gad.1063703.
69. Costa, A., Gupta, R., Signorino, G., Malara, A., Cardile, F., Biondo, C., Midiri, A., Galbo, R., Trieu-Cuot, P., Papasergi, S., et al. (2012). Activation of the NLRP3 inflammasome by group B streptococci. J. Immunol. *188*, 1953–1960. https://doi.org/10.4049/jimmunol.1102543.
70. Huet, O., Ramsey, D., Miljavec, S., Jenney, A., Aubron, C., Aprico, A., Stefanovic, N., Balkau, B., Head, G.A., de Haan, J.B., and Chin-Dusting, J.P.F. (2013). Ensuring animal welfare while meeting scientific aims using a murine pneumonia model of septic shock. Shock *39*, 488–494. https://doi.org/10.1097/SHK.0b013e3182939831.
71. Lentini, G., Famà, A., De Gaetano, G.V., Galbo, R., Coppolino, F., Venza, M., Teti, G., and Beninati, C. (2021). Role of endosomal TLRs in Staphylococcus aureus infection. J. Immunol. *207*, 1448–1455. https://doi.org/10.4049/jimmunol.2100389.
72. Biondo, C., Midiri, A., Messina, L., Tomasello, F., Garufi, G., Catania, M.R., Bombaci, M., Beninati, C., Teti, G., and Mancuso, G. (2005). MyD88 and TLR2, but not TLR4, are required for host defense against Cryptococcus neoformans. Eur. J. Immunol. *35*, 870–878. https://doi.org/10.1002/eji.200425799.

STAR★METHODS

KEY RESOURCES TABLE

REAGENT or RESOURCE	SOURCE	IDENTIFIER
Antibodies		
Purified Rat Anti-Mouse CD16/CD32 (Mouse BD Fc Block™) Clone 2.4G2 (RUO)	BD Biosciences	Cat #553142
PE Rat Anti-Mouse Ly-6G Clone 1A8	BD Biosciences	Cat #551461
PE Rat IgG2a, κ Isotype Control	BD Biosciences	Cat #553930
F4/80 Monoclonal Antibody (BM8), eFluor™ 450, eBioscience™	Invitrogen	Cat #48-4801-82
Rat IgG2a kappa Isotype Control (eBR2a), eFluor™ 450, eBioscience™	Invitrogen	Cat #48-4321-82
IL-1 beta (Pro-form) Monoclonal Antibody (NJTEN3), APC, eBioscience™	Invitrogen	Cat #17-7114-80
Rat IgG1 kappa Isotype Control (eBRG1), APC, eBioscience™	Invitrogen	Cat #17-4301-82
PE Rat Anti-Mouse CD19 Clone 1D3	BD Biosciences	Cat #553786
CD3 Monoclonal Antibody (17A2), Alexa Fluor™ 700, eBioscience™	Invitrogen	Cat #56-0032-82
Rat IgG2b kappa Isotype Control (eB149/10H5), Alexa Fluor™ 700, eBioscience™	Invitrogen	Cat #56-4031-80
CD117 (c-Kit) Monoclonal Antibody (2B8), eFluor 450	Invitrogen	Cat #48-1171-82
Rat IgG2b kappa Isotype Control (eB149/10H5), eFluor™ 450, eBioscience™	Invitrogen	Cat #48-4031-82
Ly-6G Monoclonal Antibody (1A8-Ly6g), Functional Grade, eBioscience™	Invitrogen	Cat #16-9668-82
Rat IgG2a kappa Isotype Control (eBR2a), Functional Grade, eBioscience™	Invitrogen	Cat #16-4321-82
Goat polyclonal to beta Actin- Loading Control antibody	Abcam	Cat #ab8229
Mouse IL-1 beta/IL-1F2 Antibody	R&D Systems	Cat #AF-401-NA
Phospho-RIP (Ser166) (E7G6O) Rabbit mAb	Cell Signaling technology	Cat #53286
RIP (D94C12) XP® Rabbit mAb	Cell Signaling technology	Cat #3493
Polyclonal Swine Anti-Rabbit Immunoglobulins/HRP	Dako	Code number #P0399
Polyclonal Rabbit anti-Goat IgG HRP-conjugated Antibody	R&D Systems	Cat #HAF017
Bacterial and virus strains		
Streptococcus agalactiae typing strain H36B	ATCC	ATCC 8057
Streptococcus pneumoniae serotype 2 (strain D39)	University of Siena, Italy	NCTC 7466
Klebsiella pneumoniae AC133	University of Messina, Italy	N/A
Chemicals, peptides, and recombinant proteins		
Z-IETD-FMK (Caspase-8 Inhibitor)	Sellckchem (Selleck Chemicals LLC)	Cat #S7314
Z-VAD-FMK (Pan-caspase Inhibitor)	Sellckchem	Cat #S7023
Z-YVAD-FMK (Caspase-1 Inhibitor)	Sellckchem	Cat #S8507
Dimethyl Sulfoxide (DMSO)	Sigma-Aldrich	SKU #D8418
Todd-Hewitt broth (THB)	Oxoid	Cat #CM0189
LB broth, Miller	Sigma-Aldrich	SKU #L3152
Trypticasein Soy Broth (TSB) EP/USP/ISO	Condalab	Cat #1224

(*Continued on next page*)

Continued

REAGENT or RESOURCE	SOURCE	IDENTIFIER
Industrial Agar	Condalab	Cat #1804
Trypticase Soy Agar II with 5% horse blood	BD Biosciences	REF 212099
RPMI 1640 with L-glutamine	Corning	REF 10-040-CV
Fetal Bovine Serum (FBS)	Sigma-Aldrich	SKU #F2442
Penicillin Streptomycin Solution 100X	Corning	Cat #30-002-CI
Distilled Water Sterile Tissue Culture Tested	EuroClone	Cat #ECM0970L
Dulbecco's Phosphate Buffer Saline w/o Calcium w/o Magnesium (DPBS)	EuroClone	Cat #ECB4004L
Percoll PLUS	GE Healthcare	Cod #17-5445-02
Recombinant Murine Macrophage Colony Stimulating factor (M-CSF)	PeproTech	Cat #315-02
Recombinant Murine Granulocyte-Macrophage Colony-Stimulating Factor (GM-CSF)	PeproTech	Cat #250-05
Escherichia coli K12 ultrapure LPS	InvivoGen	Cat code tlrl-peklps
Protease Inhibitor Cocktail, 50X	Promega	Cat #G6521
Ficoll®-Paque Premium	GE Healthcare, Sigma-Aldrich	SKU GE17-5442-02
Lymphoprep™	STEMCELL Technologies	Cat #07811
20X Bolt MOPS SDS Running Buffer	Invitrogen	Cat #B0001
4X Bolt™ LDS Sample Buffer	Invitrogen	Cat #B0007
10X Bolt Sample Reducing Agent	Invitrogen	Cat #B0009
Bovine Serum Albumin (BSA)	Sigma-Aldrich	SKU#A7906
Immobilon Forte Western HRP substrate	Millipore	WBLUF0100
3,3′,5,5′-Tetramethylbenzidine (TMB) Liquid Substrate System for ELISA	Sigma-Aldrich	SKU #T0440
Necrostatin-1	Sigma-Aldrich	SKU #N9037
Red Blood Cell Lysis Buffer	Roche	REF #11814389001
Recombinant Mouse IFN-β	R&D Systems	Cat #8234-MB
TaqMan™ Gene Expression Assay (FAM) Inventoried Mouse ACTB (Actin, Beta) Endogenous Control	Applied Biosystems™	Cat #4352341E
TaqMan™ Gene Expression Assay (FAM) Inventoried IL-1beta Mm00434228_m1	Applied Biosystems™	Cat #4331182
TaqMan™ Gene Expression Assay (FAM) Inventoried TNF-alpha Mm00443258_m1	Applied Biosystems™	Cat #4331182
TaqMan™ Gene Expression Assay (FAM) Inventoried Cxcl1 Mm04207460_m1	Applied Biosystems™	Cat #4331182
TaqMan™ Gene Expression Assay (FAM) Inventoried Cxcl2 Mm00436450_m1	Applied Biosystems™	Cat #4331182
TaqMan™ Gene Expression Assay (FAM) Inventoried Cxcl10 Mm00445235_m1	Applied Biosystems™	Cat #4331182
TaqMan™ Gene Expression Assay (FAM) Inventoried Ifn-1beta Mm00439552_s1	Applied Biosystems™	Cat #4331182
TaqMan™ Gene Expression Assay (FAM) Inventoried IL-6 Mm00446190_m1	Applied Biosystems™	Cat #4331182
TaqMan™ Gene Expression Assay (FAM) Inventoried IL-12b Mm01288992_m1	Applied Biosystems™	Cat #4331182
TaqMan™ Gene Expression Assay (FAM) Inventoried Actin betaHs01060665_g1	Applied Biosystems™	Cat #4331182
TaqMan™ Gene Expression Assay (FAM) Inventoried Hs00174103_m1	Critical commercial assays	Cat #4331182
Critical commercial assays		
Mouse IL-1 beta/IL-1F2 DuoSet ELISA	R&D Systems	Cat #DY401
Mouse CXCL2/MIP-2 DuoSet ELISA	R&D Systems	Cat #DY452

(*Continued on next page*)

Continued

REAGENT or RESOURCE	SOURCE	IDENTIFIER
Mouse CXCL1/KC DuoSet ELISA	R&D Systems	Cat #DY453
Mouse TNF-alpha DuoSet ELISA	R&D Systems	Cat #DY410
Mouse IL-18 DuoSet ELISA	R&D Systems	Cat #DY7625
Mouse IL-1 alpha/IL-1F1 DuoSet ELISA	R&D Systems	Cat #DY400
Proteome Profiler Mouse Cytokine Array Kit, Panel A	R&D Systems	Cat #ARY006
Bio-Plex Pro™ Human Chemokine Panel, 40-Plex	Bio-Rad	Cat #171AK99MR2
Pierce LDH Cytotoxicity Assay Kit	ThermoFisher Scientific	Cat #88954
Micro BCA™ Protein Assay Kit	ThermoFisher Scientific	Cat #23235
Pyrochrome® LAL Chromogenic Endotoxin Testing Reagent	Associates of Cape Cod, Inc.	Cat #C1500
Caspase-Glo® 8 Assay System	Promega	Cat #G8200
LIVE/DEAD Fixable Aqua Dead Cell Stain Kit, for 405 nm excitation	Invitrogen	Cat #L34957
eBioscience™ Intracellular Fixation & Permeabilization Buffer Set	Invitrogen	Cat #88-8824-00
RNeasy Mini Kit	QIAGEN	Cat #/ID: 74004
M-MLV Reverse Transcriptase	Invitrogen	Cat # 28025013
Experimental models: Organisms/strains		
Mouse: C57BL/6	Charles River Laboratories	Strain Code 027
Mouse: CD1 IGS	Charles River Laboratories	Strain Code 022
Mouse: *Casp1/11*$^{-/-}$	Max Planck Institute, Berlin, Germany	N/A
Mouse: *Ripk3*$^{-/-}$	Genentech, Inc., CA, USA	N/A
Mouse: *Ripk1* D138N	University of Cologne, Germany	N/A
Mouse: *Mlkl*$^{-/-}$	The Walter and Eliza Hall Institute of Medical Research, Australia	N/A
Mouse:*Mlkl*$^{-/-}$ *Casp8*$^{-/-}$	University Health Network, Toronto, ON, Canada	N/A
Mouse: *Ifnb1*$^{-/-}$	Lund University, Sweden	N/A
Mouse:*Myd88*$^{-/-}$	Osaka University, Japan	N/A
Mouse: *Ticam1*$^{-/-}$ (TRIF KO)	Osaka University, Japan	N/A
Mouse: *Nlrp3*$^{-/-}$	Genentech, Inc., CA, USA	N/A
Software and algorithms		
GrapdhPad Prism	GraphPad Software, Inc.	RRID:SCR_002798 (http://www.graphpad.com/)
Image Lab™ Software	Bio-Rad	Cat #1709690
i-control™Software for Infinite 200 PRO plate reader	TECAN	https://lifesciences.tecan.com/
CFX Maestro Software for CFX Real-Time PCR Instruments	Bio-Rad	Cat #12013758
FlowJo software	TreeStar	https://www.flowjo.com/
Other		
BD Trucount™ Absolute Counting Tubes	BD Biosciences	Cat #340334
Precision Plus Protein™ WesternC™ Blotting Standard	Bio-Rad	Cat #1610376
Bolt 4 to 12%, Bis-Tris Mini Protein Gel	Invitrogen	Cat #NW04120B0X
Immun-Blot PVDF Membrane	Bio-Rad	Cat #1620177
96 Well TC-Treated Microplates	Sigma-Aldrich	SKU CLS3599

(*Continued on next page*)

Continued

REAGENT or RESOURCE	SOURCE	IDENTIFIER
96-well microplates with U-bottom, cellGrade™ BRANDplates®	VWR International	Cat #781960
Corning® Costar® TC-Treated Multiple Well Plates	Sigma-Aldrich	SKUCLS3516
Corning®Costar® TC-Treated Multiple Well Plates	Sigma-Aldrich	SKU CLS3512
Corning®Costar® TC-Treated Multiple Well Plates	Sigma-Aldrich	SKUCLS3524
GentleMACS™ M Tubes	Miltenyi Biotec.	Order no. 130-093-236
GentleMACS™ Dissociator	Miltenyi Biotec.	Order no. 130-093-235
Nanodrop 2000 spectrophotometry	ThermoFisher Scientific	N/A
Bio-Rad Molecular Imager ChemiDoc™ XRS	Bio-Rad	Cat#1708265
Bio-Plex 200 Systems	Bio-Rad	Cat#171000201
Infinite® 200 PRO plate reader	TECAN	https://lifesciences.tecan.com/
BD FACSCanto™ II Clinical Flow Cytometry System	BD Biosciences	N/A
CFX96 Touch Real-Time PCR Detection System	Bio-Rad	RRID:SCR_018064

RESOURCE AVAILABILITY

Lead contact

Further information and requests for resources and reagents should be directed to and will be fulfilled by the lead contact, Giuseppe Teti (gioteti@mac.com).

Materials availability

No unique reagents were generated in this study.

Data and code availability

- All data supporting the findings of this study are available within the paper and its supplemental information files.
- This study did not generate any unique code or database.
- Any additional information required to reanalyze the data reported in this paper is available from the lead contact upon request.

EXPERIMENTAL MODEL AND SUBJECT DETAILS

Mice

Six-to eight-week-old C57BL/6 and CD1 wild-type (WT) female mice were obtained from Charles River Laboratories. Although data presented here were obtained with female mice only, sex-related differences in responses to caspase-8 inhibition were not detected in additional experiments. *Casp*1/11$^{-/-}$,[64] *Ripk3*$^{-/-}$,[65] *Mlkl*$^{-/-}$,[66] *Ifnb1*$^{-/-}$,[26,67] *Mlkl*$^{-/-}$*Casp8*$^{-/-}$,[68] *Myd88*$^{-/-}$[69], *Trif*$^{-/-}$[69] and *Nlrp3*$^{-/-}$[69] mice were all on a C57Bl/6 background. All mice were housed in individually ventilated cages under specific pathogen-free conditions in the animal facilities of the Department of Pathology of the University of Messina. All studies were performed in strict accordance with international guidelines for the use of laboratory animals and were approved by the relevant national authority (Ministero della Salute of Italy, permits n. 786/2018-PR and 112/2023-PR).

Human blood samples

Peripheral blood samples were provided by the Blood bank at St. Olavs Hospital (Trondheim, Norway). Samples were obtained from healthy volunteers providing their written informed consent according to the protocol approved by the Regional Committee for Medical and Health Research Ethics (REC Central, Norway, no. 2009/2245). Personal data management was in accordance with the General Data Protection Regulation (EU) 2016/679 (GDPR).

Bacterial strains

The GBS WT strain H36B serotype Ib[21] was used throughout the present study. *Streptococcus pneumoniae* serotype 2 strain D39 and *K. pneumoniae* AC133,[38] a carbapenem resistant strain isolated from a pneumonitis patient, were used to induce pneumonitis. GBS, *S. pneumoniae* and *K. pneumoniae* were grown in, respectively, Todd-Hewitt broth (THB), THB supplemented with 1% (v/v)

fetal calf serum (FCS), and Luria-Bertani broth (LB). All strains were grown to the mid-log phase at 37°C with 5% CO_2, washed twice in nonpyrogenic PBS (0.01 M phosphate, 0.15 M NaCl [pH 7.4]), and resuspended to the desired concentration as previously described.[21,26,38]

METHOD DETAILS

Administration of caspase inhibitors

z-IETD-fmk (caspase-8 inhibitor), z-YVAD-fmk (caspase-1/11 inhibitor) and z-VAD-fmk (pan-caspase inhibitor) dissolved in dimethysulfoxide (DMSO) to a 25 mM concentration. In most experiments, z-IETD-fmk was given to mice i.p. at a dose of 6 mg/kg of body weight. In preliminary experiments it was determined that this dose results in inhibition of caspase-8, but not caspase-1, as detected using luminescent enzyme assays (Promega) in peritoneal cells obtained from *in vivo* treated mice. Endotoxin contamination in inhibitor preparations was detected using the Pyrochrome amebocyte lysate test.

Mouse infections and septic shock models

To induce GBS infection, mice were challenged i.p. with 5×10^7 CFU, or i.v. with 5×10^6 CFU. Endotoxic shock was induced by an i.p. injection of LPS (40 mg/kg of body weight). To induce pneumonitis, mice were challenged with *S. pneumoniae* (1×10^8 CFU/mouse) or *K. pneumoniae* (5×10^7 CFU/mouse) by the intranasal route, as described.[38] Peritoneal lavage fluid (PLF), blood and organ homogenates were obtained and analyzed for CFU numbers, cell counts and cytokine determinations as previously described.[38,58] Peritoneal lavage fluid was obtained by injecting 2 mL of buffered saline in the peritoneal cavity and subsequently aspirating a total of 1.7–1.9 mL of fluid. Unconcentrated PLF samples were used to measure cytokine levels. After challenge, animals were observed for the development of clinical signs. Disease severity was assessed using a scoring system (mouse clinical assessment score for sepsis or M-CASS) based on pre-defined clinical criteria and humane endpoints, as described.[70] Animal showing signs of irreversible disease underwent euthanasia.

In vitro cell stimulation

Bone marrow derived neutrophils and macrophages were obtained from the femurs and tibias of 6–8-week-old female mice as previously described.[21,71] Purity of neutrophil preparations was >97%, as assessed by flow cytometry. Peritoneal cells were obtained from peritoneal lavage fluid (PLF) samples by centrifugation at 400 × g for 15 min. Relative proportions of various cell types in a representative sample are reported in Table S2. For *in vitro* stimulation experiments, cells were seeded in microtiter plates at a concentration of 5×10^5 per well in 0.2 mL of RPMI medium with 10% fetal calf serum. When indicated, peritoneal cells were pre-treated *in vitro* with recombinant IFN-β (10 pg/mL) at 2 h before the addition of z-IETD-fmk (50 μM) or vehicle. Cells were then cultured for the indicated length of time in the presence of z-IETD-fmk or vehicle. Cytokine and mRNA levels were measured in culture supernatants and cell pellets, respectively, by ELISA and Real-Time PCR as described below.

Cytokine determinations

Samples were assayed using the Pierce LDH cytotoxicity assay kit (Thermo Fisher Scientific) or for cytokine/chemokine concentrations using the following assays (all from R&D Systems): Proteome Profiler Mouse Cytokine Array Kit; CXCL1/KC DuoSet; CXCL2/MIP-2 DuoSet; TNF-α DuoSet; IL-1βDuoSet; IL-1αDuoSet; IL-18 DuoSet. The lower detection limits of these assays were 15.6 (IL-1β, IL-1α, CXCL1 and 2), 31.3 (TNF-α) and 46.9 pg/mL (IL-18). In selected experiments, cytokines were measured in PLF or peritoneal cell cultures obtained from neutrophil-depleted mice. Neutrophil depletion was achieved by i.v. injection of 100 μg of rat monoclonal anti-mouse Ly-6G Ab (clone 1A8) or rat IgG2a control (isotype control) at 24 h before z-IETD-fmk (6 mg/kg, i.p.) or vehicle treatment for 4 h in the absence of other stimuli. Under these conditions, anti–Ly6G was sufficient to reduce neutrophil blood and peritoneal counts to <1% at 24 h after treatment (Table S3). For gene expression measurements, total RNA was extracted from 4 x10^6 PLF cells, bone marrow neutrophils or macrophages and retrotranscribed. Expression of the genes encoding IL-1β, Cxcl1, Cxcl2, Cxcl10, IL-6, IFN-β, IL12b and TNF-α was determined by qPCR using a CFX96 Touch Real-Time PCR Detection System (Bio-Rad), exactly as described previously.[72] For human leukocyte studies, cytokine levels in culture supernatants were determined using the Bio-Plex Pro Human Chemokine Panel as per the manufacturer's instructions.

Western blot analysis

Peritoneal cell lysates were analyzed exactly as described.[21,71] Briefly, peritoneal cells were collected from mice at 4 h after i.p. injection with z-IETD-fmk or vehicle, washed three times with ice-cold PBS and lysed by vigorous vortexing in RIPA lysis buffer [50 mM Tris·HCl, pH 7.5, 100 mM NaCl, 1% Triton X-100, 20% glycerol, 1× protease inhibitor cocktail]. Lysates were then centrifuged at 13,000 × g for 15 min at 4°C to eliminate cellular debris. Protein concentration in each sample was determined using the Micro BCA Protein Assay Kit. Protein samples (30 μg of protein per lane) were run on precast Bolt Bis-Tris 4-12% gels with 1x MOPS buffer and transferred on PVDF (polyvinylidene difluoride) membranes. Membranes were washed in TBS-T (Tris-Buffered Saline with 0.1% Tween 20) and blocked with TBS-T containing 5% bovine serum albumin (BSA) for 2 h. Membranes were subsequently incubated with primary antibodies in TBS-T containing 1% BSA at 4°C overnight. The following primary antibodies were used: phospho-RIP (Ser166) (E7G6O) rabbit mAb, RIP (D94C12) XP rabbit mAb, anti-mouse IL-1 beta/IL-1F2 antibody and anti-beta actin. After

incubation, membranes were washed with TBS-T and incubated with secondary antibody (anti-rabbit or anti-goat IgG HRP-linked antibodies) for 2 h at room temperature in TBS-T containing 1% BSA. Protein bands were visualized by Immobilon Forte Western HRP substrate and detected using a Bio-Rad's ChemiDoc XRS system. Beta-actin was used as loading control.

Immuno-staining and flow cytometric analysis

Peritoneal cells were collected from mice at the indicated times after various treatments, washed three times with DPBS and stained in the dark for 20 min with LIVE/DEAD Fixable Aqua Dead Cell Stain Kit, according to the manufacturer's instructions. Cells were then blocked with 0.5 μg Fc Block for 20 min at room temperature and stained for surface markers for 20 min in the dark with rat anti-mouse Ly-6G (clone 1A8), rat anti-mouse F4/80 (Clone BM8), anti-mouse pro-IL-1 beta (cloneNJTEN3) or isotype control monoclonal antibodies, as described.[21,71] For intracellular staining, the Intracellular Fixation & Permeabilization Buffer Set was used, following the manufacturer's instruction. Briefly, cells were incubated for 30 min in the dark with IC Fixation Buffer and washed twice with Permeabilization Buffer 1X (Perm Buffer). Cells were then stained with the anti-mouse IL-1 beta (Pro-form) Monoclonal Antibody (clone NJTEN3) APC for 30 min in the dark at 4°C. Following two washes with Perm Buffer, cells were resuspended in PBS and 100,000 events per sample were collected on a FACS Canto II flow cytometer (BD Biosciences). Data analysis was performed using FlowJo version 10 software. For enumeration of peritoneal cells, BD Trucount Absolute Counting Tubes were used. The gating strategy for flow cytometry analyses is shown in Figure S5A.

QUANTIFICATION AND STATISTICAL ANALYSIS

Survival data were analyzed by Kaplan-Meier survival plots. All other data were analyzed by the Mann–Whitney test. Differences were considered significant when p values were less than 0.05.

Cell Reports Medicine, Volume *4*

Supplemental information

Caspase-8 inhibition improves the outcome of bacterial infections in mice by promoting neutrophil activation

Germana Lentini, Agata Famà, Giuseppe Valerio De Gaetano, Francesco Coppolino, Ahlem Khachroub Mahjoub, Liv Ryan, Egil Lien, Terje Espevik, Concetta Beninati, and Giuseppe Teti

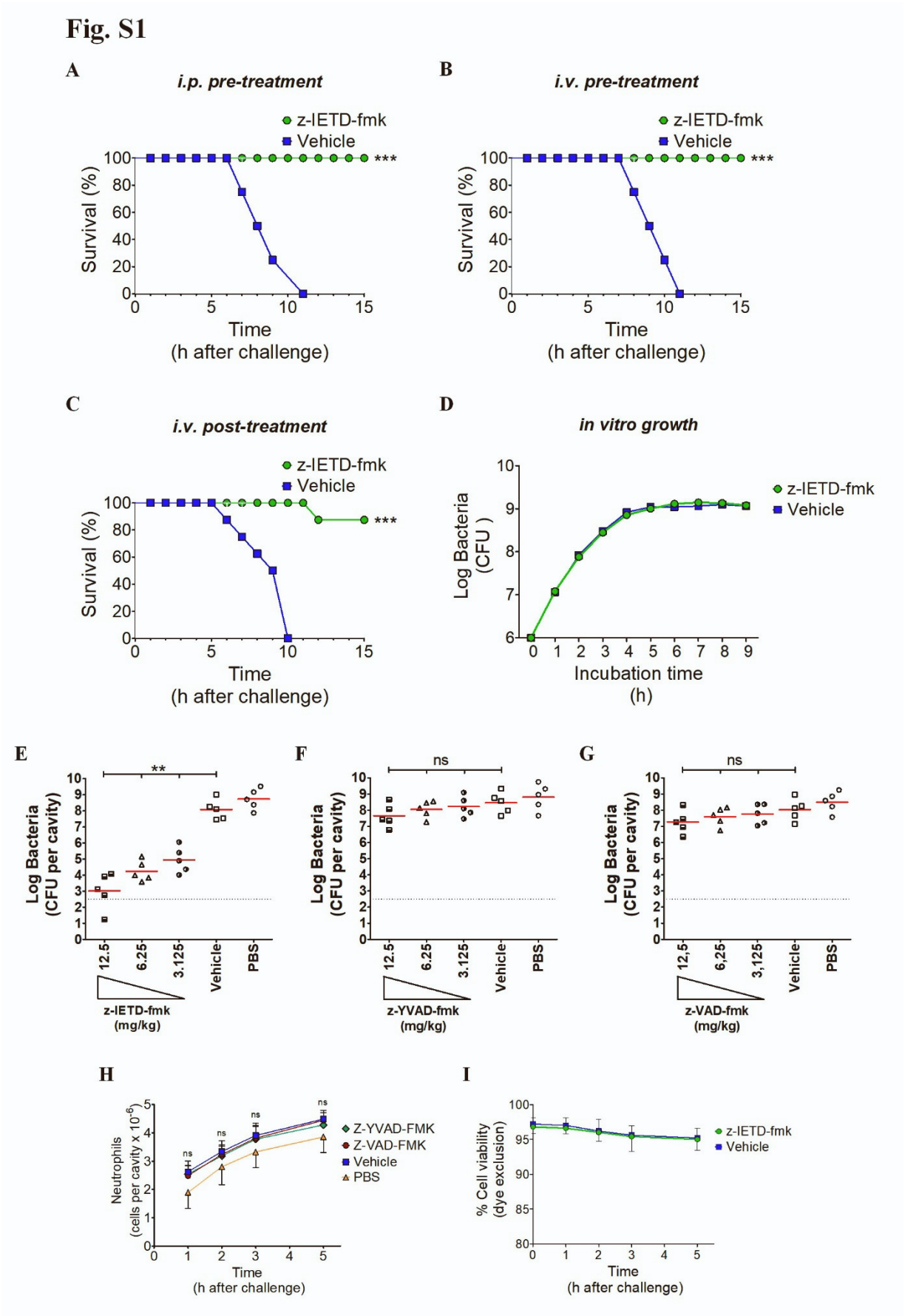

Fig. S1. Therapeutic effects of z-IETD-fmk administration in lethal peritonitis induced by group B streptococci.

Related to Figure 1. (A) Survival of mice pre-treated i.p. with z-IETD-fmk (6 mg/kg) or vehicle at 4 h before GBS

challenge (4 x107 CFU/mouse, i.p.). (B) Survival of mice pre-treated i.v. with z- IETD-fmk (6 mg/kg) or vehicle at 4 h before GBS challenge (4 x107 CFU/mouse, i.p.). (C) Survival of mice post-treated i.v. with z-IETD-fmk (6 mg/kg) or vehicle at 4 h after GBS challenge (4 x107 CFU/mouse, i.p.). Shown are cumulative data from two experiments, each involving 4 animals per group. ***, $P < 0.001$ versus vehicle-treated mice, as determined by Kaplan-Meier analysis. (D) Log CFU numbers of GBS growing in Todd Hewitt broth in the presence of z-IETD-fmk (2 mg/ml) or vehicle at the indicated times after incubation at 37°C. Data are duplicate determinations from one representative experiment of three showing similar results. (E-G) Log CFU numbers in PLF samples of mice treated with different concentrations (12.5 to 3 mg/kg, i.p.) of z-IETD-fmk (caspase-8 inhibitor; E), z-YVAD-fmk (caspase-1 inhibitor; F), or z-VAD-fmk (pan-caspase inhibitor; G) at 4 h before GBS challenge (4 x107 CFU/mouse, i.p.). PLF samples were collected at 2 h after challenge. Horizontal bars indicate mean values. The dashed lines indicate the limit of detection of the test. Each determination was conducted on a different animal during one experiment involving five animals per group. **, $P < 0.01$; ***, versus vehicle-treated mice, as determined by the Mann–Whitney U test; ns, not significant. (H) Kinetics of neutrophil influx in the peritoneal cavity after challenge with GBS (4 x107 CFU/mouse, i.p.) in animals that were pretreated with z-YVAD-fmk (12 mg/kg) or z-VAD-fmk (12 mg/kg) at 4 h before GBS challenge. (I) Cell viability in PLF samples obtained from mice treated with z-IETD-fmk (6 mg/kg, i.p.) or vehicle for the indicated times in the absence of other stimuli. Each determination was conducted on a different animal during one experiment involving five animals per group. ns, not significant, as determined by the Mann–Whitney U test.

Fig. S2

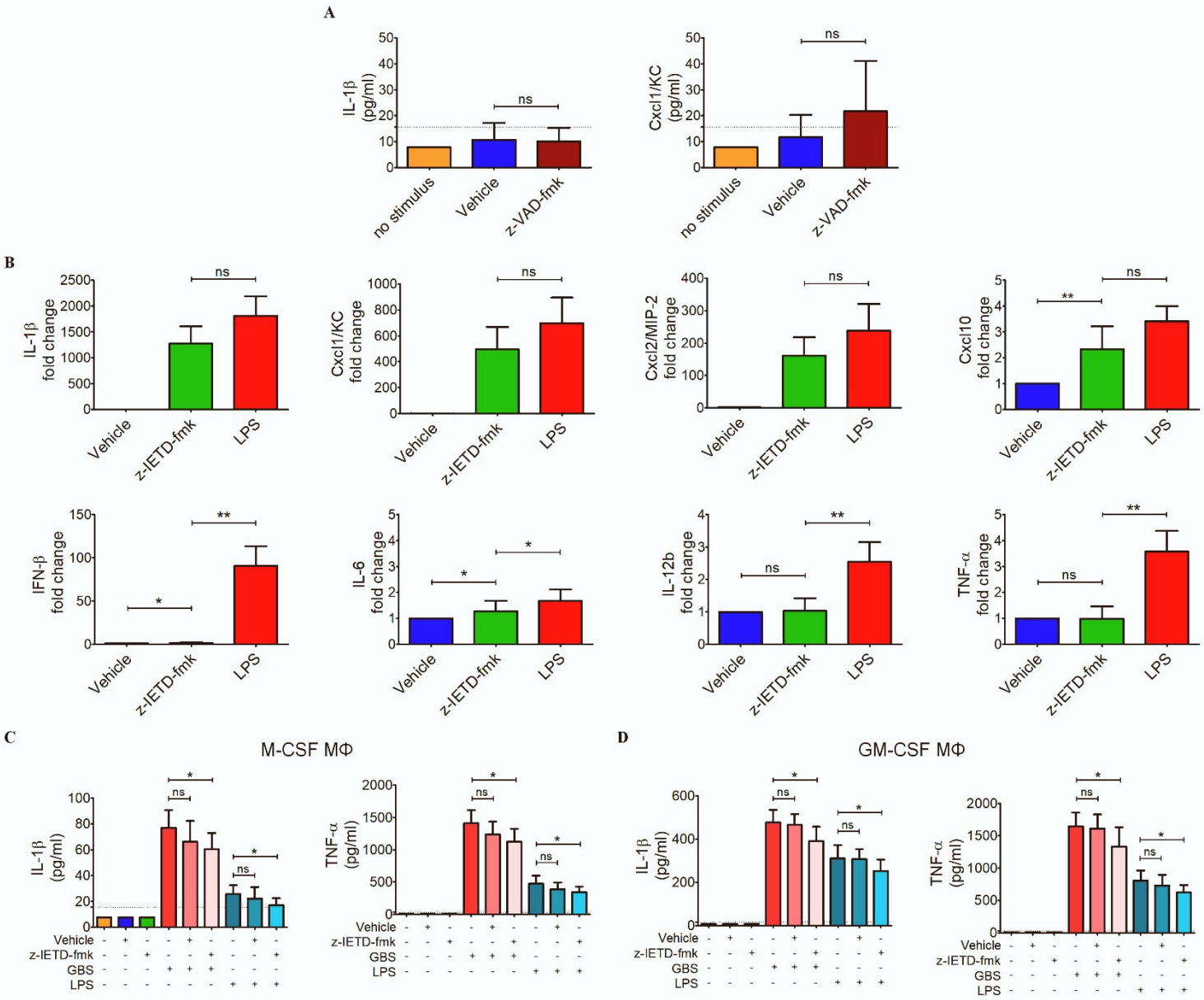
A
IL-1β (pg/ml)
Cxcl1/KC (pg/ml)
ns
no stimulus
Vehicle
z-VAD-fmk
B
IL-1β fold change
Cxcl1/KC fold change
Cxcl2/MIP-2 fold change
Cxcl10 fold change
IFN-β fold change
IL-6 fold change
IL-12b fold change
TNF-α fold change
Vehicle
z-IETD-fmk
LPS
C
M-CSF MΦ
D
GM-CSF MΦ
IL-1β (pg/ml)
TNF-α (pg/ml)
Vehicle
z-IETD-fmk
GBS
LPS

Fig. S2. Cytokine responses to z-IETD-fmk stimulation. **Related to Figure 2.** (A) IL-1β and Cxcl1 concentrations in PLF samples collected at 4 h after *in vivo* treatment with the pan-caspase inhibitor z-YVAD-fmk (12 mg/kg, i.p.) or vehicle in the absence of other stimuli. Each determination was conducted on a different animal in the course of one experiment involving five animals per group. (B) Relative mRNA expression levels of IL-1β, Cxcl1, Cxcl2, Cxcl10, IFN-β, IL-6, IL-12b and TNF-α in peritoneal cells obtained from mice at 2 h after treatment with z-IETD-fmk (6 mg/kg, i.p.), LPS (0.5 μg/kg), or vehicle. Each determination was conducted on a different animal in the course of one experiment involving five animals per group. (C and D) IL-1β and TNF-α concentrations in supernatants from cultures of M-CSF- (C) or GM-CSF-polarized (D) BMDMs after pre-treatment for 4 h with z-IETD-fmk (50 μM) or vehicle followed by stimulation with live GBS (MOI 20) or LPS (10 ng/ml). Data are means + SD from five independent experiments conducted in duplicate. *, $P < 0.05$; **, $P < 0.01$, as determined by the Mann–Whitney U test; ns, not significant.

Fig. S3

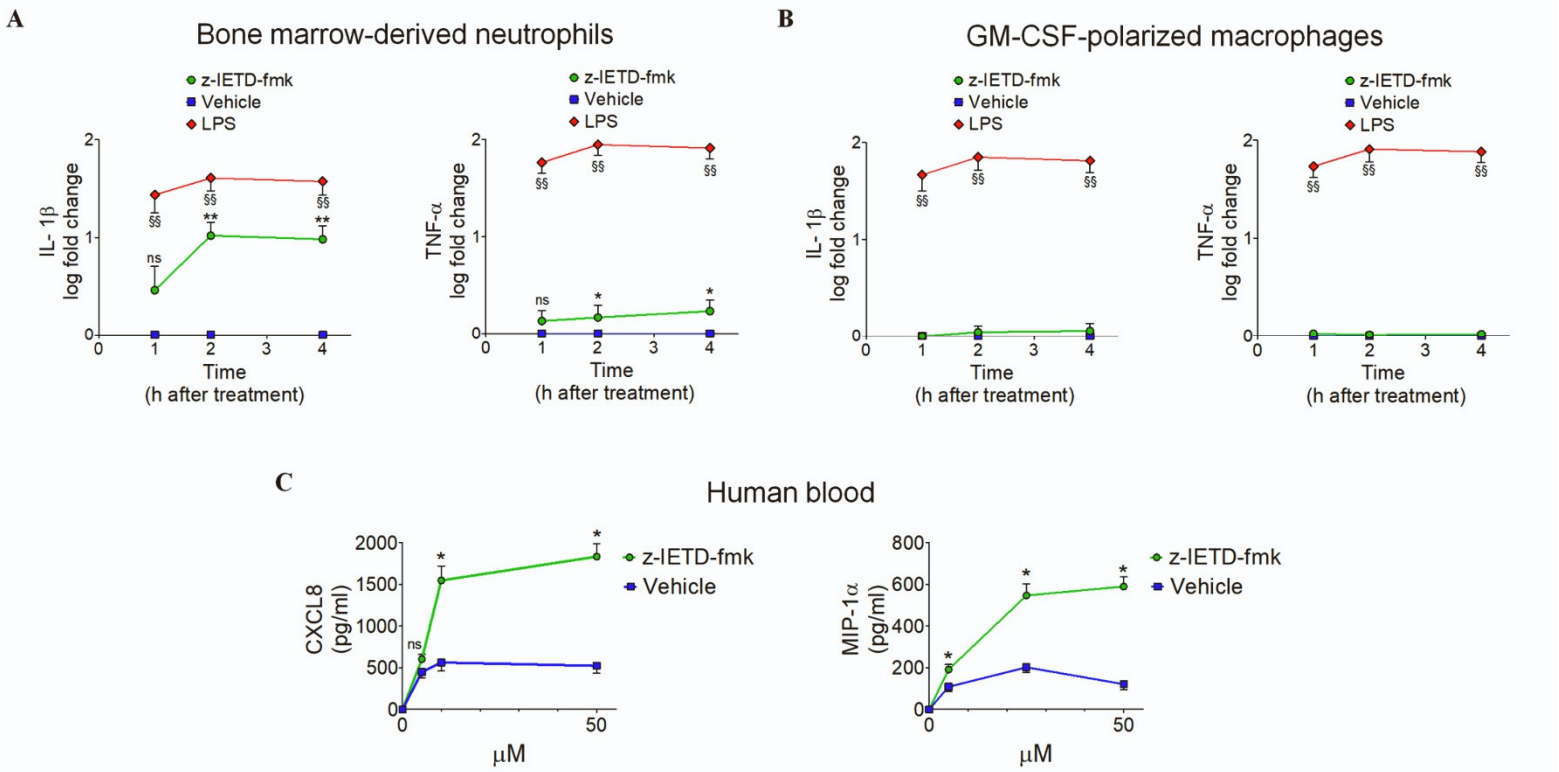

Fig. S3. Murine and human leukocytes produce cytokines in response to *in vitro* stimulation with IETD. **Related to Figure 3.** (A and B) Kinetics of relative IL-1β- or TNF-α mRNA expression levels in bone marrow-derived neutrophils (A) or GM-CSF-polarized BMDMs (B) after exposure to z-IETD-fmk (50 μM), LPS (10 ng/ml) or vehicle for the indicated times before RNA extraction. *, $P < 0.05$; **, $P < 0.01$ by Mann–Whitney U test analysis of differences between z-IETD-fmk and vehicle. §§$P < 0.01$ by Mann–Whitney U test analysis of differences between LPS and vehicle. (C) Peripheral blood was collected from a healthy volunteer and incubated with the indicated concentrations of z-IETD-fmk or DMSO vehicle at 37° C for 4 h. Plasma concentrations of CXCL8 (interleukin-8) and MIP-1α (macrophage inflammatory protein 1 alpha) were measured using the Bio-Plex Pro Human Chemokine Panel. Results are representative of 2 experiments each performed using a different donor.

Fig. S4

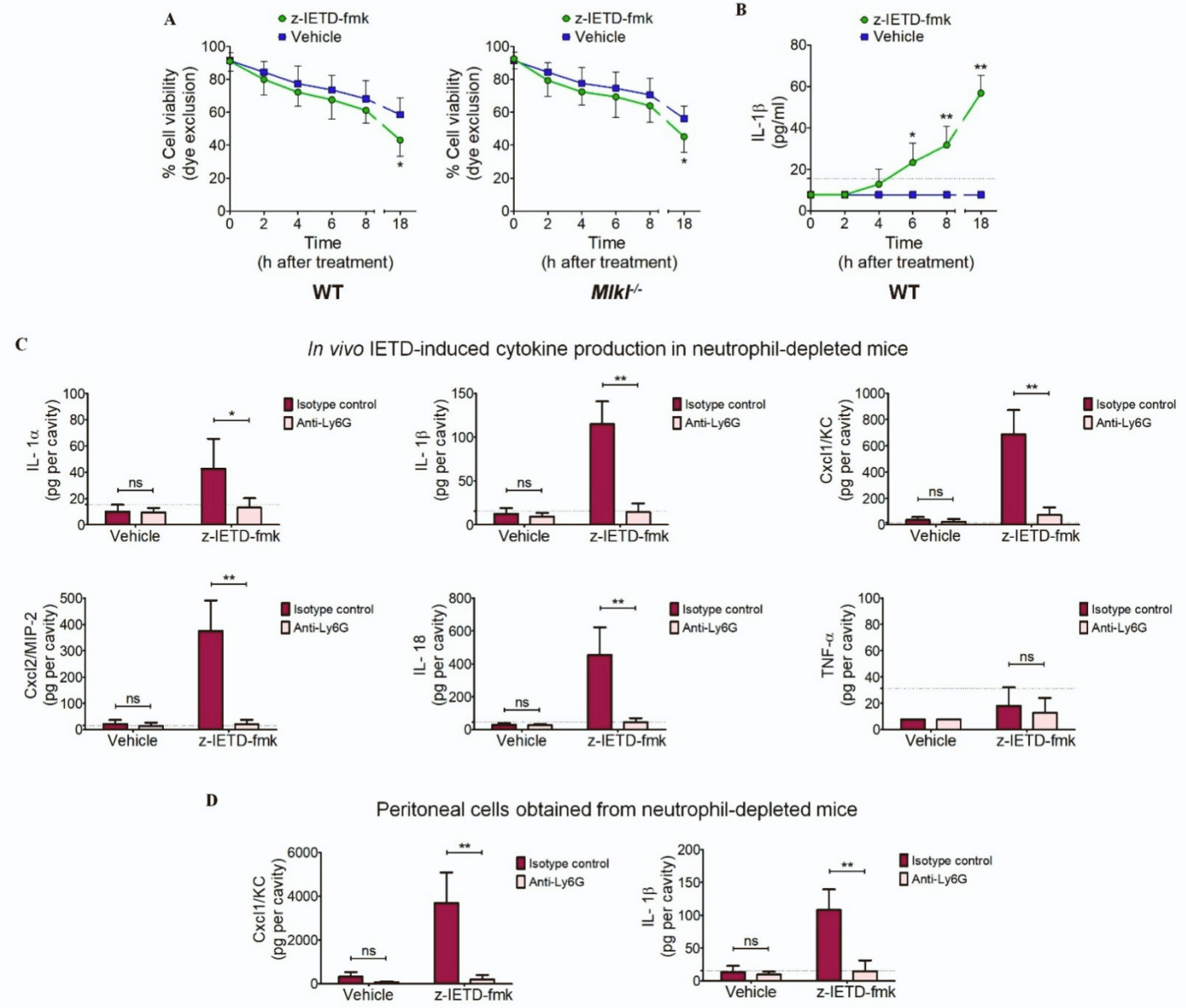
A
z-IETD-fmk
Vehicle
% Cell viability (dye exclusion)
Time (h after treatment)
WT
Mlkl-/-
B
IL-1β (pg/ml)
Time (h after treatment)
WT
C
In vivo IETD-induced cytokine production in neutrophil-depleted mice
Isotype control
Anti-Ly6G
IL- 1α (pg per cavity)
IL- 1β (pg per cavity)
Cxcl1/KC (pg per cavity)
Cxcl2/MIP-2 (pg per cavity)
IL- 18 (pg per cavity)
TNF-α (pg per cavity)
Vehicle
z-IETD-fmk
ns
D
Peritoneal cells obtained from neutrophil-depleted mice

Fig. S4. Neutrophils are a major source of cytokines after z-IETD-fmk stimulation. Related to Figure 4. (A) Spontaneous cell death in bone marrow neutrophils cultured *in vitro* in the presence of z-IETD-fmk (50 μM) or DMSO vehicle. Cells were obtained from wild type (WT) or *Mlkl*-/- mice. (B) Release of IL-1β in bone marrow neutrophils at various times during culture in the presence of z-IETD-fmk (50 μM) or DMSO vehicle. (C) Cytokine concentrations in PLF samples collected from neutrophil-depleted mice at 4 h after i.p. administration of z-IETD-fmk (6 mg/Kg) or DMSO vehicle. Mice were pretreated with anti-Ly6G mAb or control IgG (both 100 μg/mouse i.p.) at 24 h before z-IETD-fmk administration. PLF supernatants were assayed for concentration of the indicated cytokines by ELISA. (D) Mice were treated with anti-Ly6G mAb or control IgG (both 100 μg/mouse i.p.) at 24 h before collection of PLF samples. Peritoneal cells were then cultured overnight in the presence of z- IETD-fmk (50 μm) or vehicle and culture supernatants were assayed for concentration of the indicated cytokines by ELISA. Shown are means + standard deviations of results obtained from 5 duplicate determinations, each conducted on a sample obtained from a different animal. *, $P < 0.05$; **, $P < 0.01$, as determined by the Mann–Whitney U test; ns, not significant.

Fig. S5

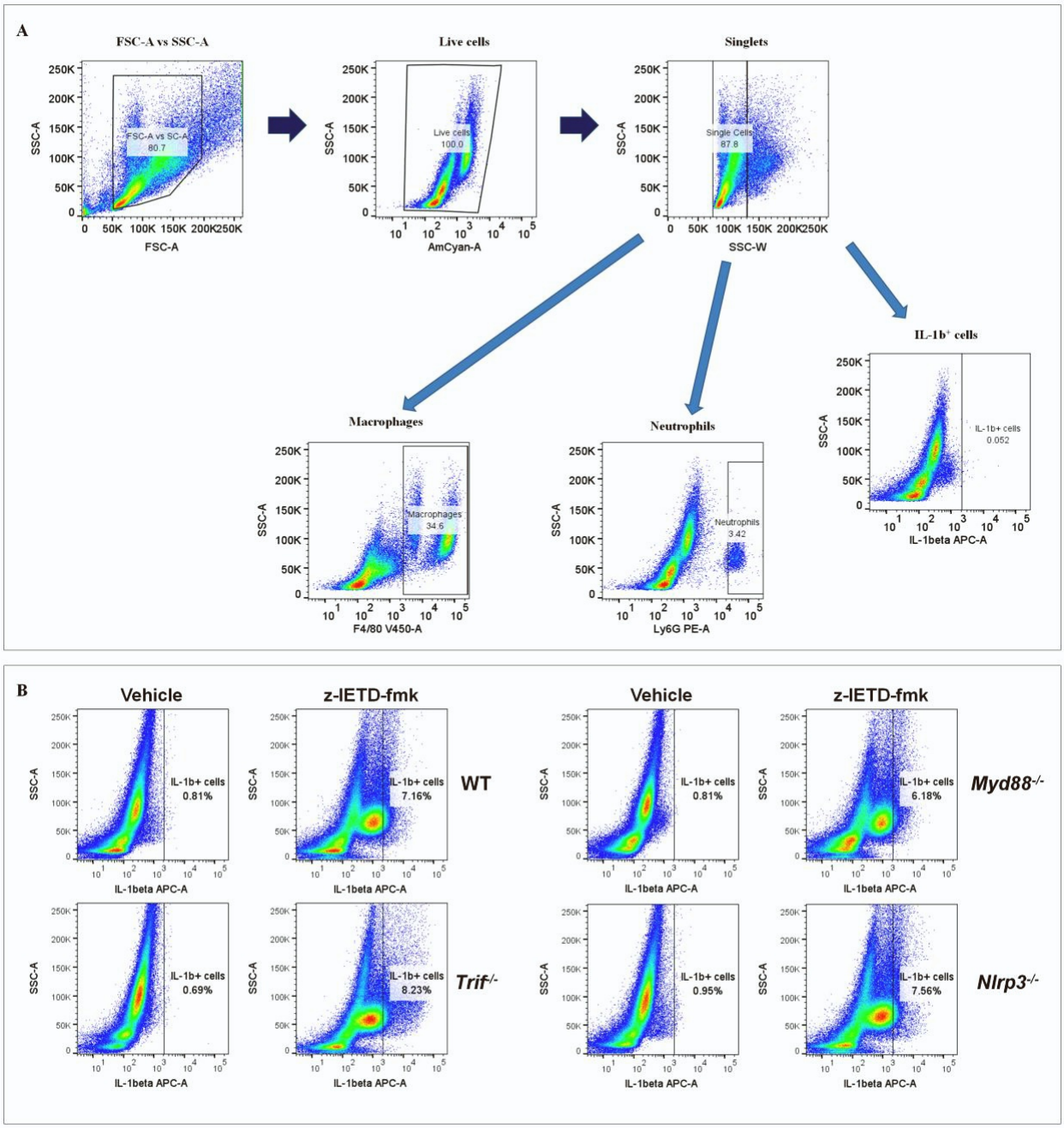

Fig. S5. z-IETD-fmk-induced IL-1β responses are not dependent on Myd88, TRIF or Nlrp3. **Related to Figure 4.** (A) Gating strategy for the identification of Ly6G+ (neutrophils), F4/80+ (macrophages), and IL-1b+ (IL-1β-producing) cells. Shown is a population of PLF cells collected from an unmanipulated mouse. In the IL-1b+ panel to the right, cells were stained with an anti-IL1β isotype control. (B) Percentages of IL-1β+ cells after intracellular staining for IL-1β in peritoneal cells obtained from WT, Myd88$^{-/-}$, Trif$^{-/-}$, or Nlrp3$^{-/-}$ mice at 2 h after treatment with z-IETD-fmk (6 mg/kg, i.p.) or vehicle in the absence of other stimuli. Data from one experiment of three showing similar results.

Fig. S6

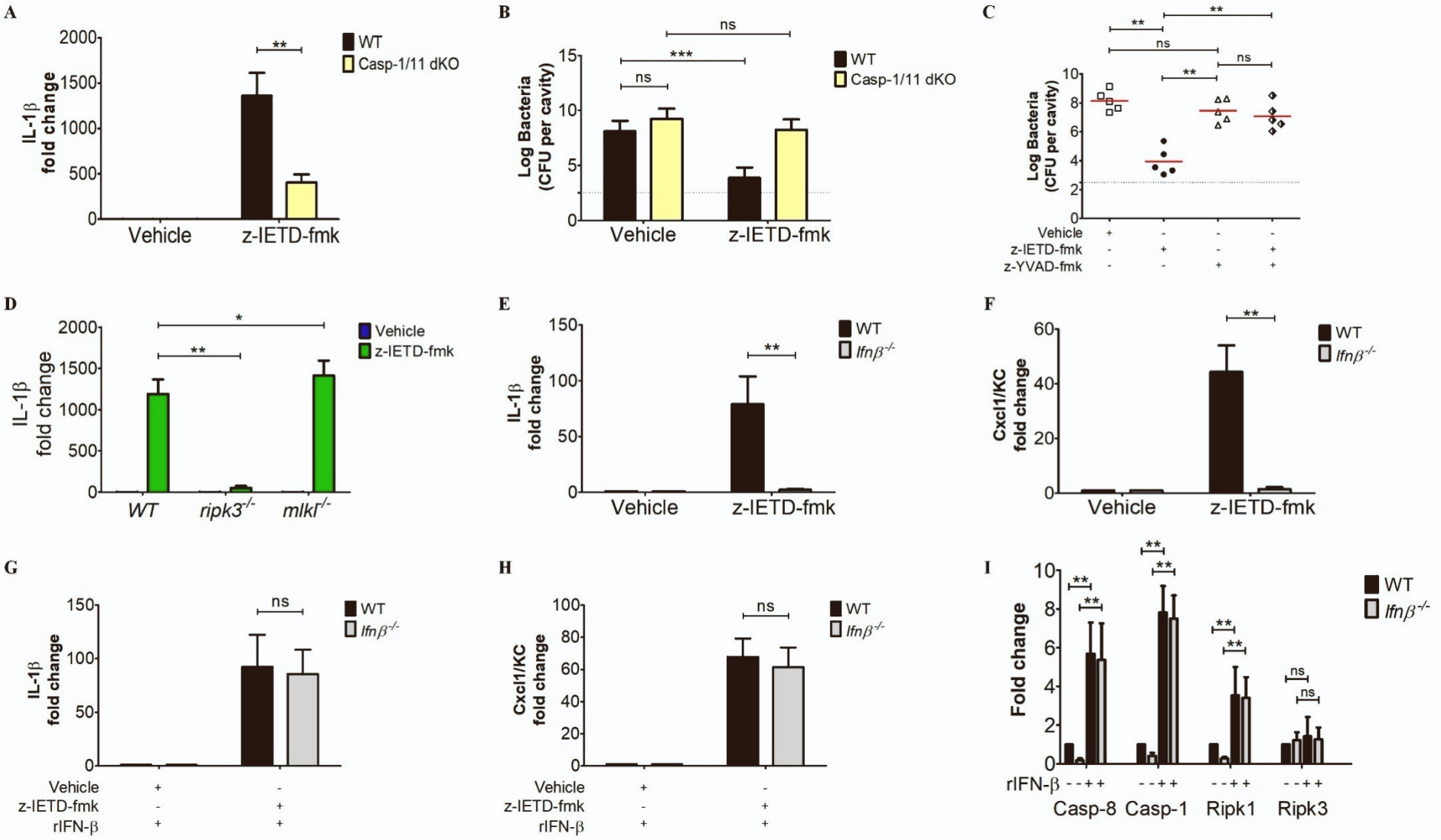
A
IL-1β fold change
2000
1500
1000
500
0
**
WT
Casp-1/11 dKO
Vehicle
z-IETD-fmk
B
Log Bacteria (CFU per cavity)
15
10
5
0
ns
***
ns
WT
Casp-1/11 dKO
Vehicle
z-IETD-fmk
C
Log Bacteria (CFU per cavity)
10
8
6
4
2
0
**
ns
**
ns
**
Vehicle + - - -
z-IETD-fmk - + - +
z-YVAD-fmk - - + +
D
IL-1β fold change
2000
1500
1000
500
0
*
**
Vehicle
z-IETD-fmk
WT
ripk3-/-
mlkl-/-
E
IL-1β fold change
150
100
50
0
**
WT
Ifnβ-/-
Vehicle
z-IETD-fmk
F
Cxcl1/KC fold change
60
40
20
0
**
WT
Ifnβ-/-
Vehicle
z-IETD-fmk
G
IL-1β fold change
150
100
50
0
ns
WT
Ifnβ-/-
Vehicle + -
z-IETD-fmk - +
rIFN-β + +
H
Cxcl1/KC fold change
100
80
60
40
20
0
ns
WT
Ifnβ-/-
Vehicle + -
z-IETD-fmk - +
rIFN-β + +
I
Fold change
10
8
6
4
2
0
**
**
**
**
**
**
ns
ns
WT
Ifnβ-/-
rIFN-β - - + + - - + + - - + + - - + +
Casp-8
Casp-1
Ripk1
Ripk3

Fig. S6. Caspase-1/11 and IFN-β are required for transcriptional responses to z-IETD-fmk. Related to Figures 5 and 6. (A) Relative IL-1β mRNA expression levels in peritoneal cells from WT or caspase-1/11-/- mice at 2 h after i.p. administration of z-IETD-fmk (6 mg/kg) or vehicle in the absence of other stimuli. (B) Log CFU numbers in PLF samples from WT or caspase-1/11-/- mice pre-treated with z-IETD-fmk (6 mg/kg i.p.) or vehicle at 4 h before GBS challenge (4 x107 CFU/mouse, i.p.). (C) Log CFU numbers in PLF samples obtained from mice treated with vehicle, z-IETD-fmk (6 mg/kg i.p), z-YVAD-fmk (6 mg/kg i.p.), or a combination of these inhibitors at 4 h before GBS challenge (4 x107 CFU/mouse, i.p.). PLF samples were collected at 2 h after bacterial challenge. Horizontal bars indicate mean values. The dashed lines indicate the limit of detection of the test. (D) Relative IL-1β mRNA expression levels in peritoneal cells from WT, RIPK3-/- or MLKL-/- mice at 2 h after z-IETD-fmk (6 mg/kg i.p.) or vehicle administration in the absence of other stimuli. Each determination was conducted on a different animal in the course of one experiment involving five animals per group. (E and F) Relative IL-1β (E) and Cxcl1 (F) mRNA expression levels in peritoneal cells obtained from WT or IFN-β-/- mice and stimulated *in vitro* with z-IETD-fmk (50 μM) or vehicle for 2 h. (G and H) Relative IL-1β (G) and Cxcl1 (H) mRNA expression levels in *in vitro* cultured peritoneal cells from WT or IFN-β-/- mice pre-treated with recombinant IFN-β (10 pg/ml) at 2 h before the addition of z- IETD-fmk (50 μM) or vehicle. (I) Relative expression of caspase-8, caspase-1, RIPK1 or RIPK3 in unstimulated peritoneal cells from WT or IFN-β-/- mice. Where indicated, cells were treated with recombinant IFN-β (10 pg/ml) for 2 h. Reference values, observed in untreated WT cells, were given a value of 1. Shown are means + standard deviations of duplicate determinations conducted on five separate samples, each obtained from a different mouse. *, $P < 0.05$; **, $P < 0.01$, ***, $P < 0.001$ as determined by the Mann–Whitney U test; ns, not significant.

Fig. S7

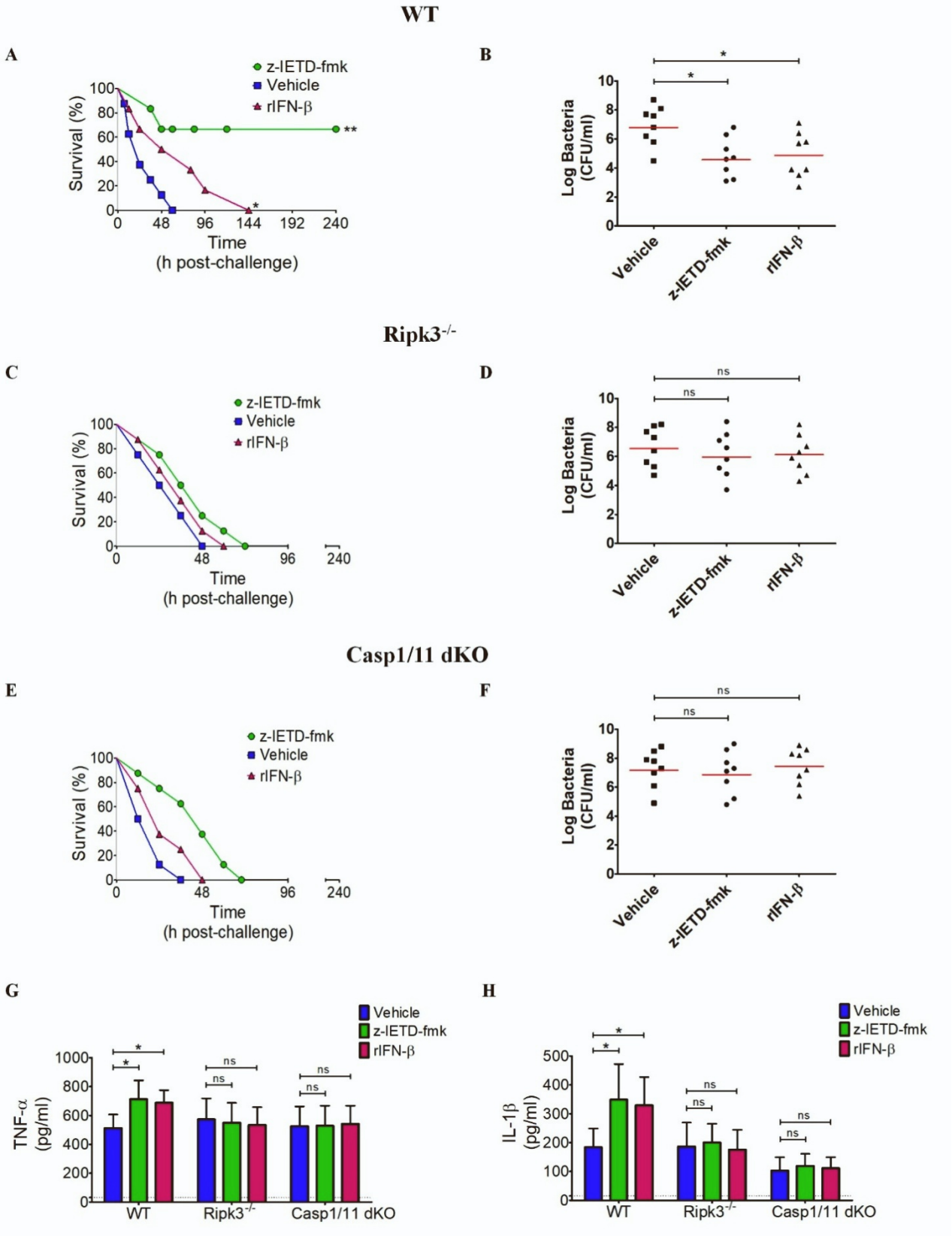

Fig. S7. Protective effect of z-IETD-fmk in a septic shock model involving i.v. challenge with live bacteria. **Related to Figures 5 and 6.** Wild type, Ripk3$^{-/-}$ or caspase-1/11$^{-/-}$ (Casp1/11dKO) mice were treated with z-IETD-fmk

(6 mg/kg, i.v.), vehicle or recombinant IFN-β (6 ×104 IUs, i.p.) at 1h before i.v. challenge with live GBS (5 x 106 CFU/mouse). (A, C, and E) Survival curves showing cumulative data from two experiments, each involving 8 animals per group. *, $P < 0.05$; **, $P < 0.01$, versus vehicle-treated mice, as determined by Kaplan-Meier analysis. (B, D, and F) Log CFU numbers in the blood at 24 h after infection. (G and H) Blood TNF-α (G) and IL-1β (H) levels at 24 h post-challenge with live GBS. *, $P < 0.05$ versus vehicle-treated mice, as determined by the Mann–Whitney U test.

Coordinate	Target/Control	Alternate Nomenclature
A1, A2	Reference spot	—
A23, A24	Reference spot	—
B1, B2	BLC	CXCL13/BCA-1
B3, B4	C5/C5a	Complement component 5a
B5, B6	G-CSF	—
B7, B8	GM-CSF	—
B9, B10	I-309	CCL1/TCA-3
B11, B12	Eotaxin	CCL11
B13, B14	sICAM-1	CD54
B15, B16	IFN-γ	—
B17, B18	IL-1α	IL-1F1
B19, B20	IL-1β	IL-1F2
B21, B22	IL-12ra	IL-1F3
B23, B24	IL-2	—
C1, C2	IL-3	—
C3, C4	IL-4	—
C5, C6	IL-5	—
C7, C8	IL-6	—
C9, C10	IL-7	—
C11, C12	IL-10	—
C13, C14	IL-13	—
C15, C16	IL-12p70	—
C17, C18	IL-16	—
C19, C20	IL-17	—
C21, C22	IL-23	—
C23, C24	IL-27	—
D1, D2	IP-10	CXCL10/CRG-2
D3, D4	I-TAC	CXCL11
D5, D6	KC	CXCL1
D7, D8	M-CSF	—
D9, D10	JE	CCL2/MCP-1
D11, D12	MCP-5	CCL12
D13, D14	MIG	CXCL9
D15, D16	MIP-1α	CCL3
D17, D18	MIP-1β	CCL4
D19, D20	MIP-2	CXCL2
D21, D22	RANTES	CCL5
D23, D24	SDF-1	CXCL12
E1, E2	TARC	CCL17
E3, E4	TIMP-1	—
E5, E6	TNF-α	—
E7, E8	TREM-1	—
F1, F2	Reference spot	—
F23, F24	PBS (Negative Control)	—

Table S1. Related to Figure 2. Mouse cytokine array coordinates.

Cell types	Percentages (%)
B lymphocytes	23.4 - 64.6
Macrophages	29.7 - 47.4
T lymphocytes	4.1 - 4.3
Dendritic cells	2.3 - 5.3
Neutrophils	1.9 – 3.5
Mast cells	0.4 – 1.9
Other cells	1.0 – 5.0

Table S2. **Related to STAR Methods.** Percentages of cell subsets in the peritoneal fluid of an unmanipulated mouse.

Treatment	Blood	Peritonealfluid
Control IgG	5.9 ± 1.1	2.5 ± 0.6
Anti-Ly6G	0.3 ± 0.2	0.2 ± 0.1

Table S3. **Related to STAR Methods.** Effect of 24h anti-Ly6G treatment on blood or peritoneal polymorphonuclear leukocytes counts.